

2000 CEDAR Workshop
Boulder, Colorado
June 25-30, 2000

Tutorial Lecture

by Stephen Bougher
University of Arizona

**Comparative Terrestrial Planet Thermospheres:
Venus, Earth, and Mars**

CEDAR WORKSHOP 2000
COMPARATIVE TERRESTRIAL PLANET THERMOSPHERES:
VENUS, EARTH, AND MARS

I. Introduction

- Basic fundamental planetary parameters and implications
- Hierarchy of model development at NCAR (1975-present)

II. Basic Features of Structure and Dynamics of Thermospheres

- Vertical temperature structure and global mean composition (over solar cycle)
- Common thermospheric processes and possible thermostatic controls
- EUV/UV energy deposition and heating efficiencies
- Auroral and joule heating
- 1-D global mean heat balances and implications
- Global scale wind patterns

III. Recent (V-M) Thermospheric Data Illustrating Key Features

- Venus and Mars upper atmosphere sampling over past 25 years
- Solar cycle (rotational) responses of thermospheric temperatures
- Compositional variations (horizontal) from data and empirical models
- Storm responses : Mars (dust forcing)
- Mars planetary waves : MGS discovery of longitude fixed waves (diurnal Kelvin wave explanation)

IV. TGCM Modeling Tools (Venus, Earth, and Mars)

- Descriptions of the VTGCM, TIEGCM, and MTGCM
- Common inputs for equinox and solstice, solar cycle simulations

V. TGCM (V-E-M) Simulations for Equinox Conditions

- Global temperature, composition, and wind distributions (homopause and exobase)
- Solar cycle variations of same
- Dayside heat balances (radiative and dynamical)
- Time dependent variation of dayside composition and temperatures
- Role of CO₂-O cooling as a thermostat controlling temperatures
- Role of global dynamics as a thermostat controlling temperatures

VI. TGCM (E-M) Simulations for Solstice Conditions

- Global temperature, composition, and wind distributions (homopause and exobase)
- Seasonal plus solar cycle variations of same
- Role of orbital eccentricity impacting temperatures
- Mars lower atmosphere dust impacts on its thermosphere (coupling of atmospheric regions)

VII. Summary and Conclusions

- Key comparative planetary thermosphere problems
- UA website archive of TGCM results

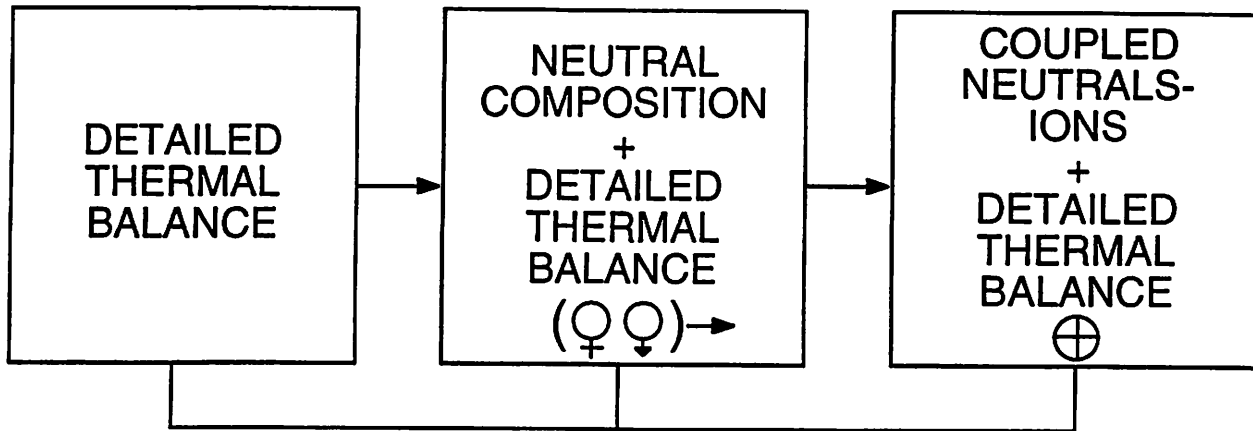
Table 1a. Terrestrial Planet Parameters

Parameter	Earth	Venus	Mars
Gravity, cm/s ²	982	888	373
Heliocentric distance AU	1.0	0.72	1.38-1.67
Radius, km	6371	6050	3396
Ω , rad/s	7.3(-5)	3.0(-7)	7.1(-5)
Magnetic dipole moment (wrt Earth)	1.0	$\leq 4.0(-5)$	$\leq 2.5(-5)$
Obliquity, deg	23.5	1-3	25.0

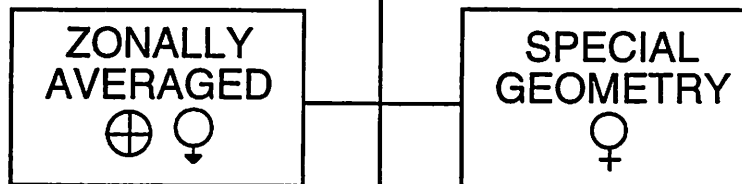
Table 1b. Implications of Parameters

Effect	Earth	Venus	Mars
Scale heights, km	10-50	4-12	8-22
Major EUV heating, km	~ 200 -300 broad	~ 140 -160 narrow	120-160 intermediate
O Abundance (ion peak)	$\sim 40\%$	~ 7 -20%	~ 1 -4%
CO ₂ 15- μ m cooling	≤ 130 km	≤ 160 km	≤ 125 -130 km
Dayside thermostat	conduction	CO ₂ cooling	winds/conduction
Dayside solar cycle T	900-1500 K	230-310 K	220-325 K
Rotational forces	important	negligible	important
Cryosphere	no	yes	no
Auroral/Joule heating	yes	no	no
Seasons	yes	no	yes

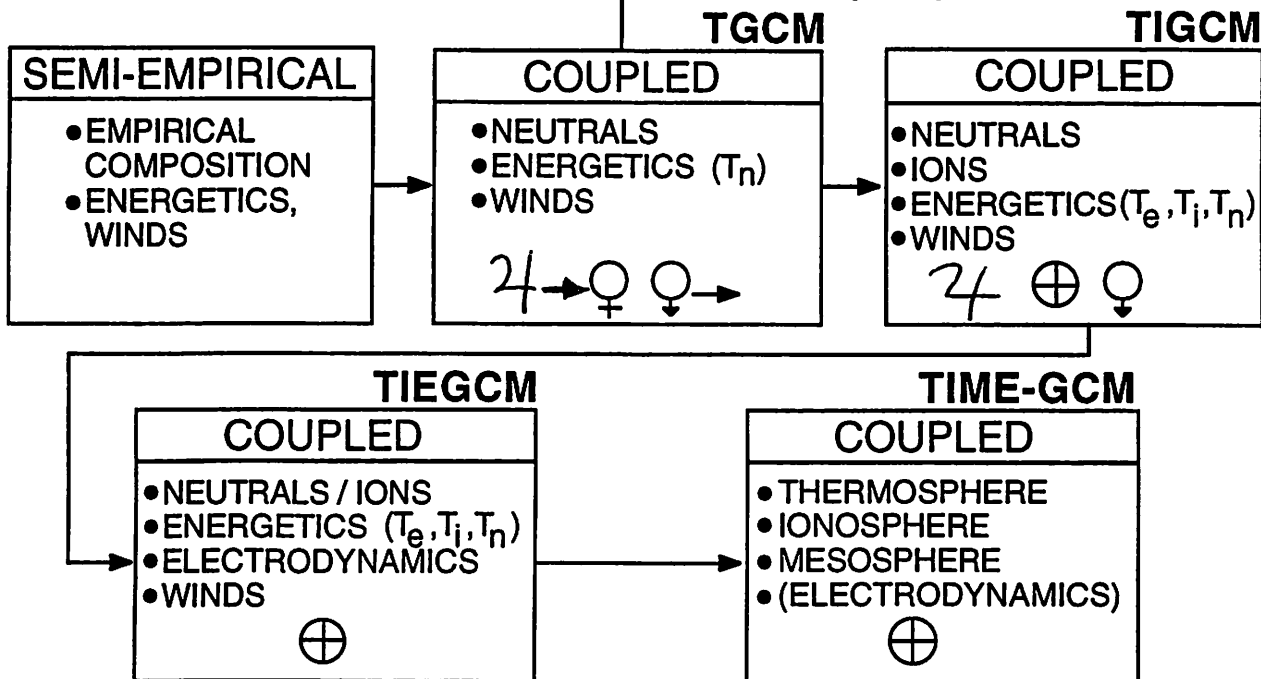
ONE DIMENSIONAL GM MODELS (1D)



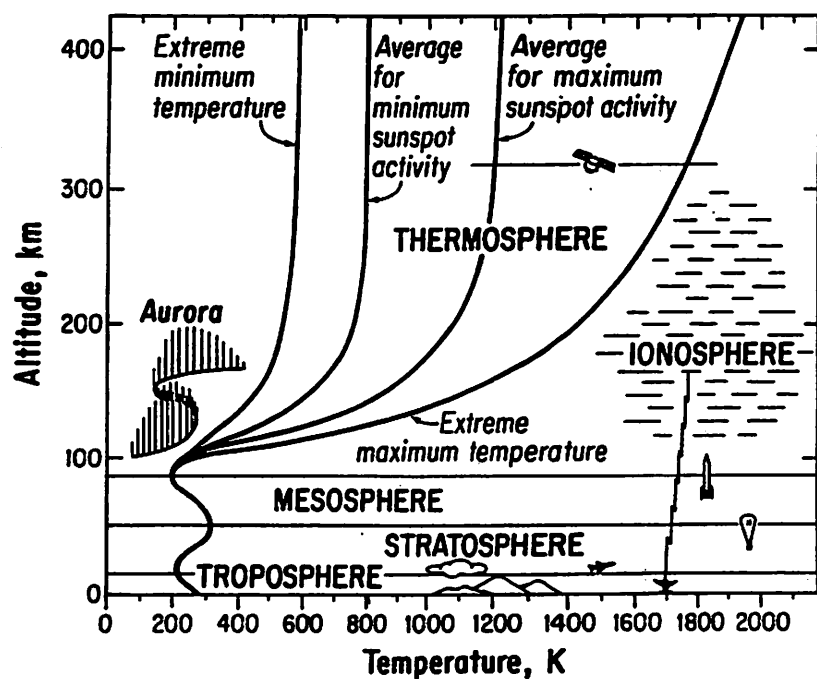
SIMPLIFIED DYNAMICAL MODELS (2D)



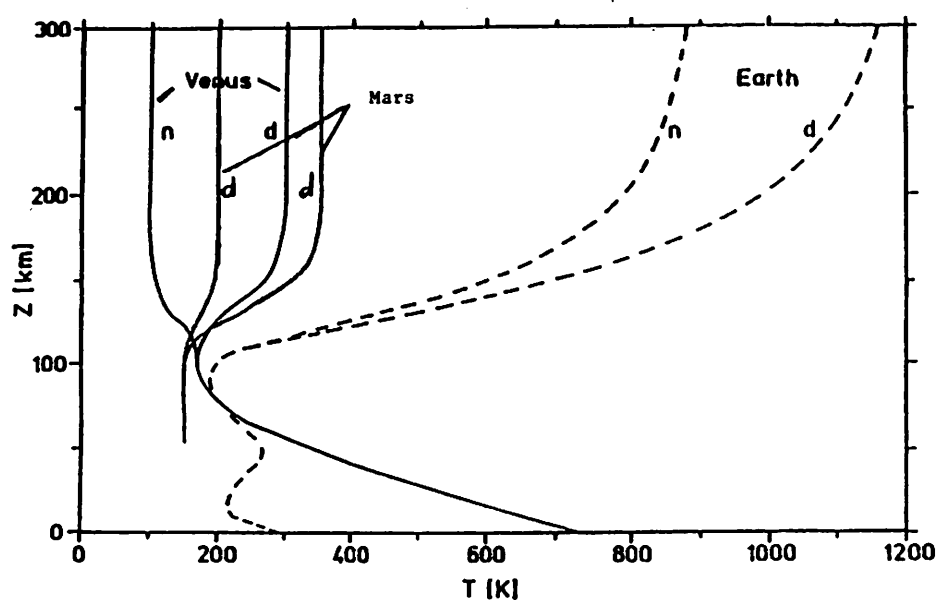
GLOBAL MODELS (3D)



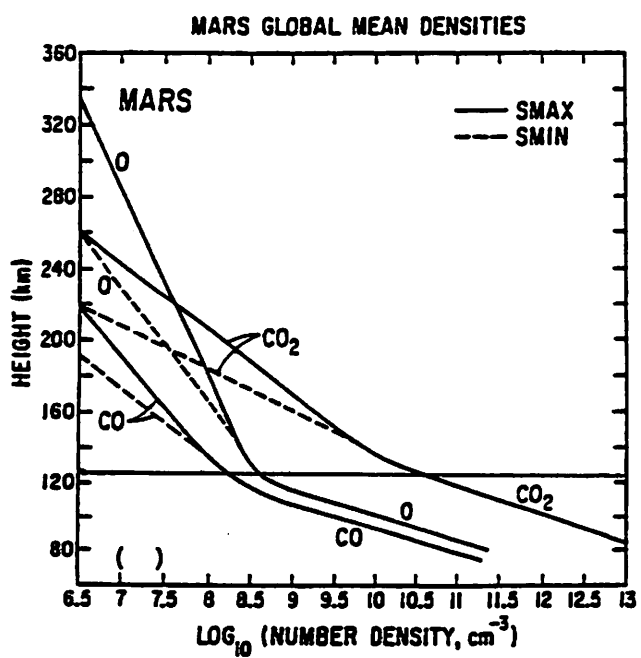
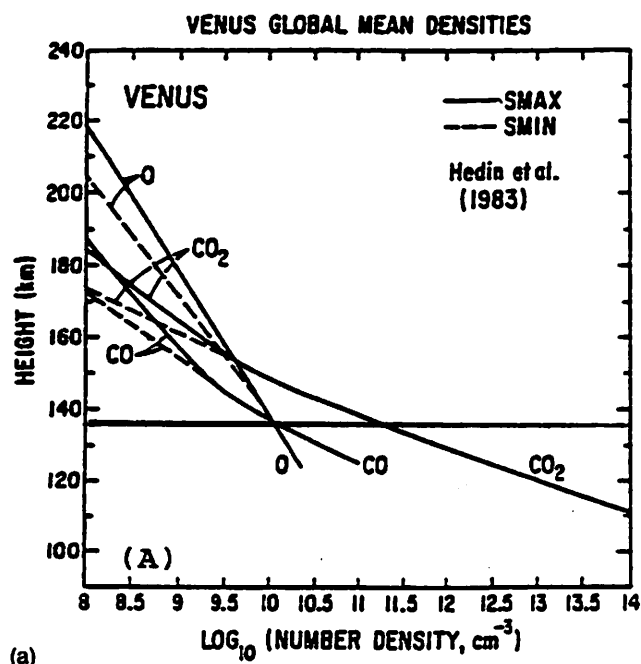
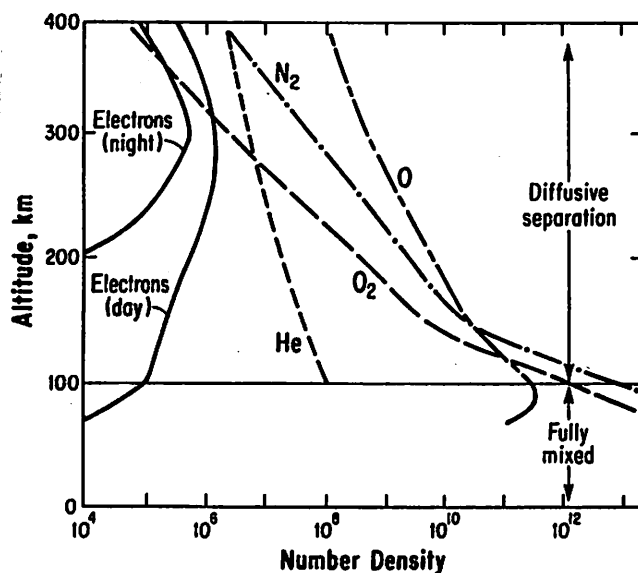
Bouger and Roble (97)



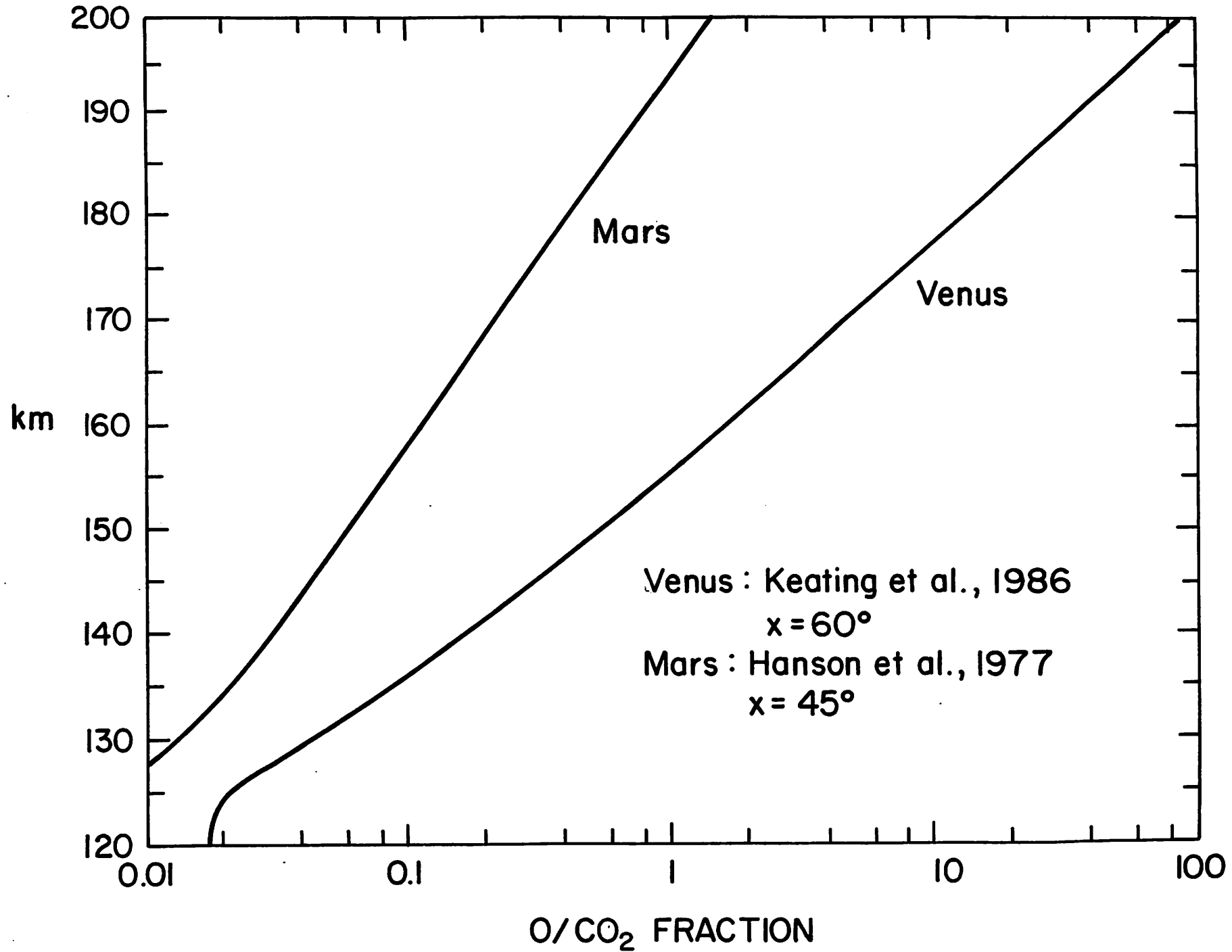
Fox and Bouger (91)



Bougher and Roble (97)



O/CO₂ MIXING RATIO : VENUS AND MARS



COMMON (UNIQUE) THERMOSPHERIC PROCESSES

- HEATING

- Solar EUV/UV heating (1.0-225.0 nm)
- Solar near-IR heating (1.0-4.3 microns) (Venus and Mars)
- Auroral/Joule heating (Earth)
- Tidal heating and/or GW dissipation
- Dynamical (advection/compression) heating

- COOLING

- Molecular thermal conduction
- Eddy thermal conduction (Venus and Mars)
- CO₂ IR cooling at 15-microns
 - (Main IR radiator at mesopause heights)
 - (Enhanced by atomic-O collisions)
- NO(5.3-microns) (Earth)
 - (Importance presently under debate)
- Dynamical (advection/expansion) cooling

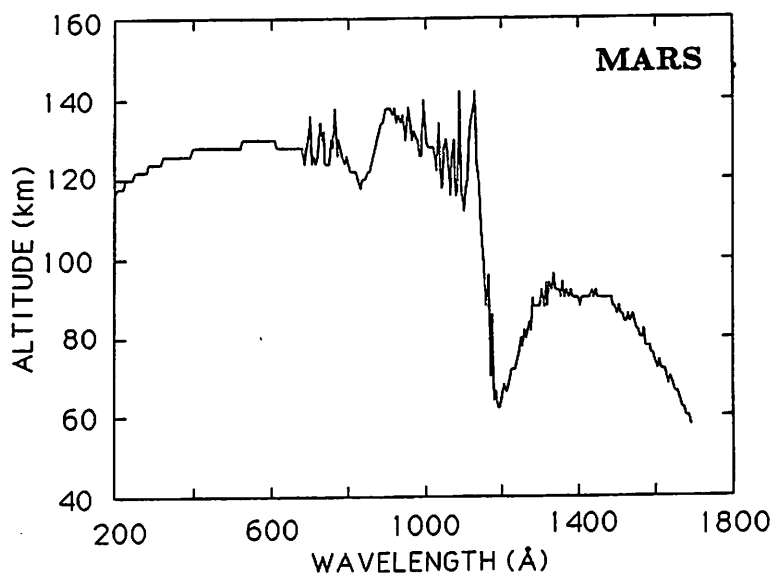
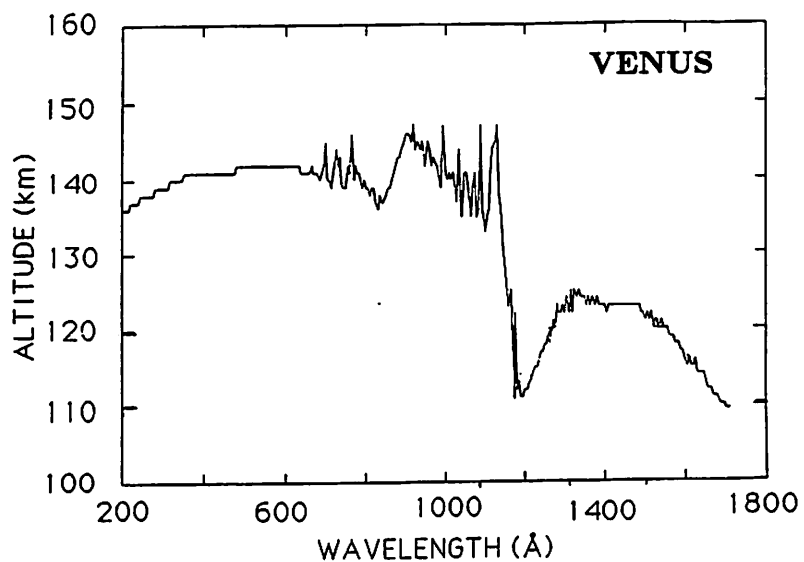
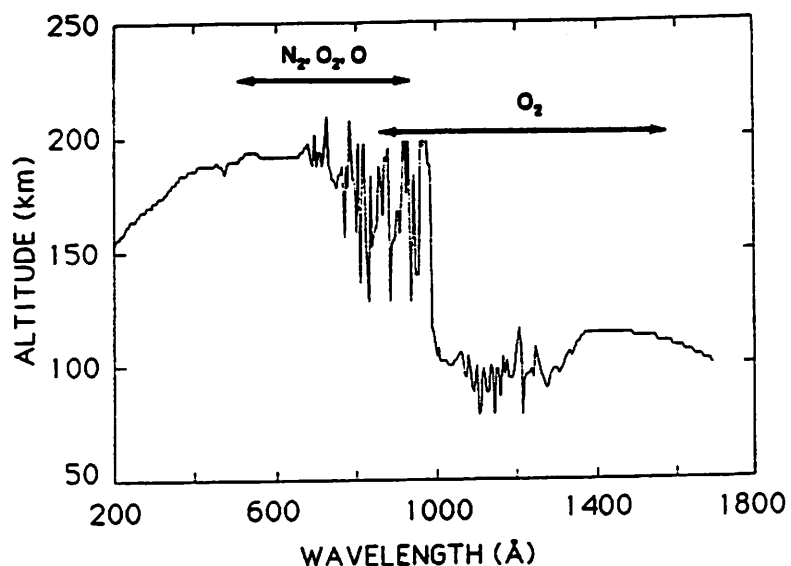
- CONSTITUENTS

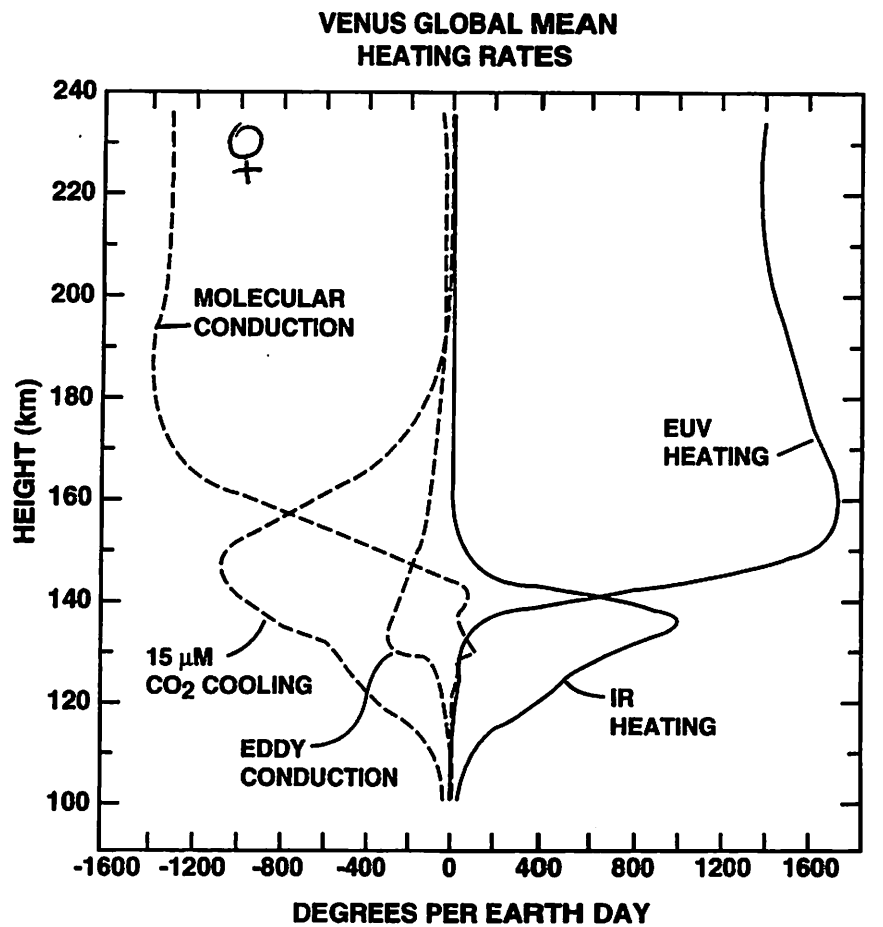
- O₂ and N₂ dominated atmosphere (Earth)
- CO₂ dominated atmosphere (Venus and Mars)
- Chemical sources and sinks
- Molecular vs. eddy diffusion
- Hydrostatics and redistribution by global winds
- Exospheric escape
- Downward fluxes into lower atmosphere (Earth, others?)

- WINDS

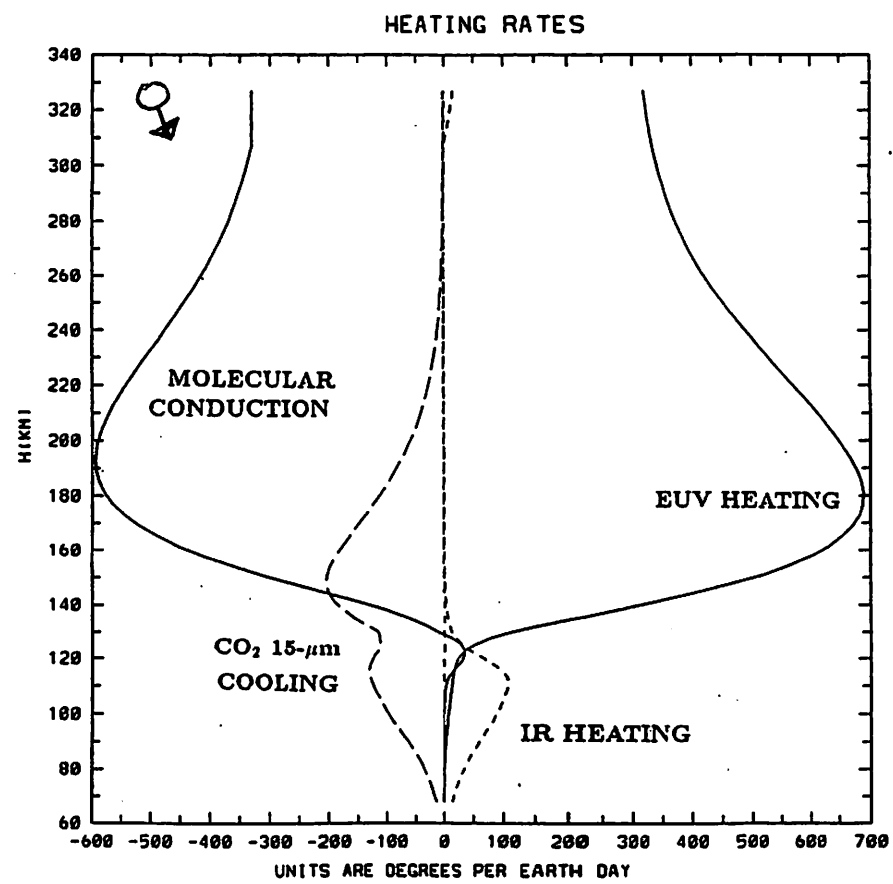
- Neutral pressure gradient driven
- Molecular and eddy viscosity
- Hydrodynamic advection; non-linear terms
- Coriolis torques (Earth and Mars)
- Gravity wave drag (Venus)
- Ion drag (Earth)
- Tidal forcing of MLT region (Earth and Mars)

Paxton and Anderson (92)





Bouger et al., (94)



Fox (88)

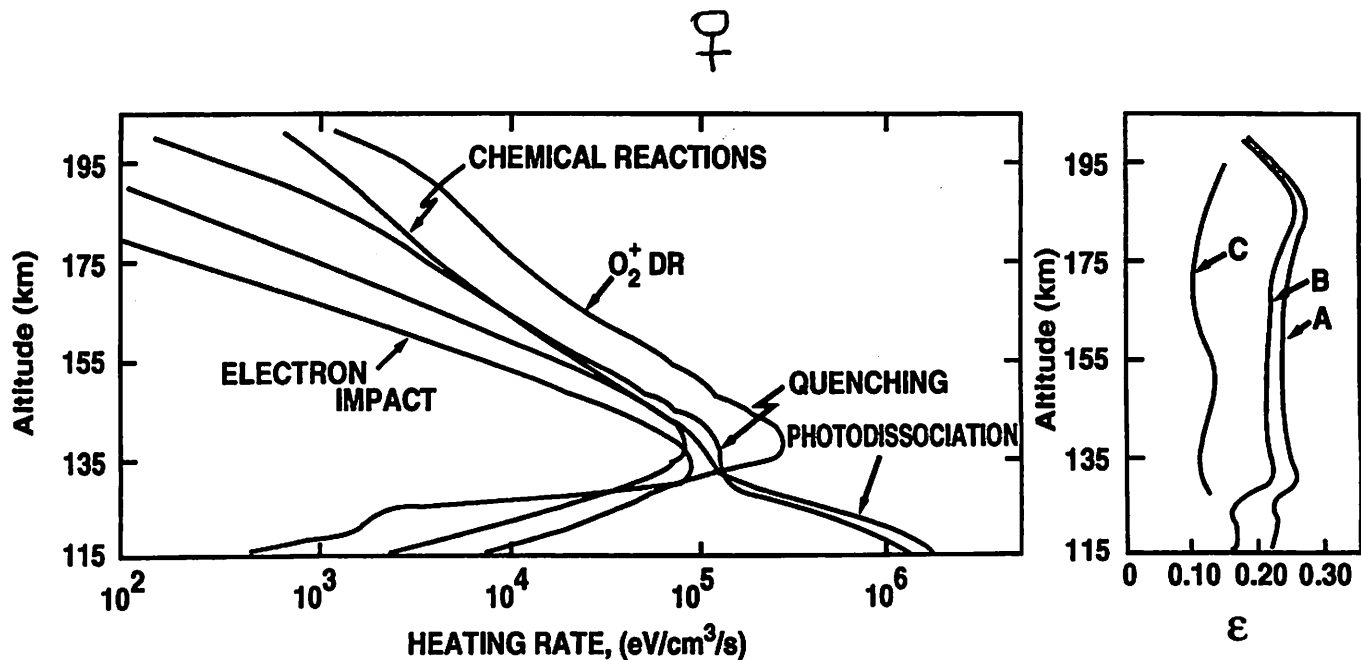
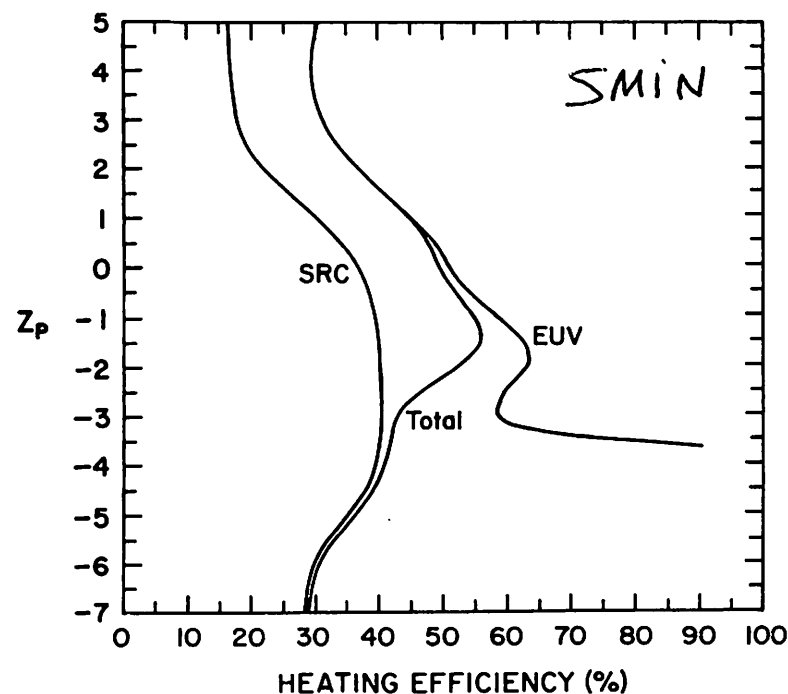
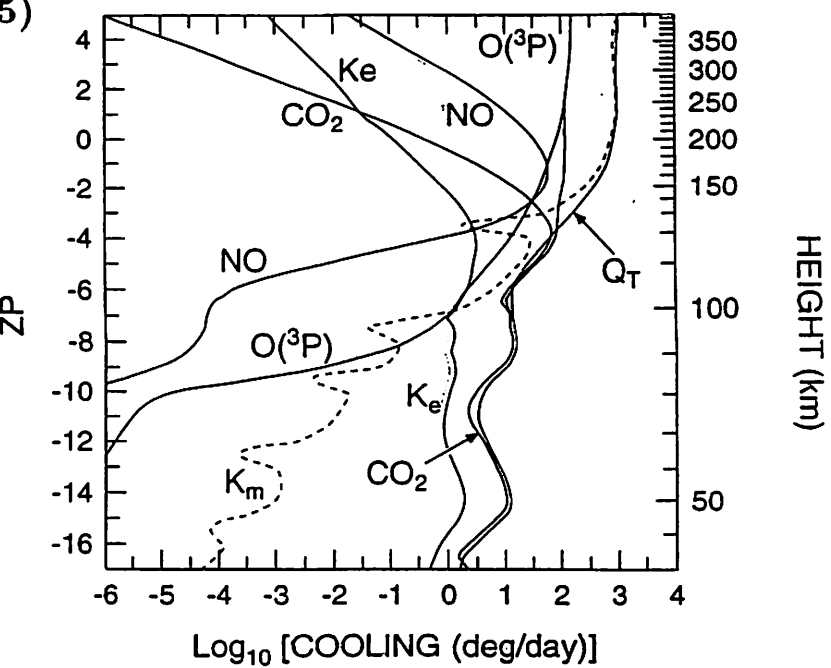
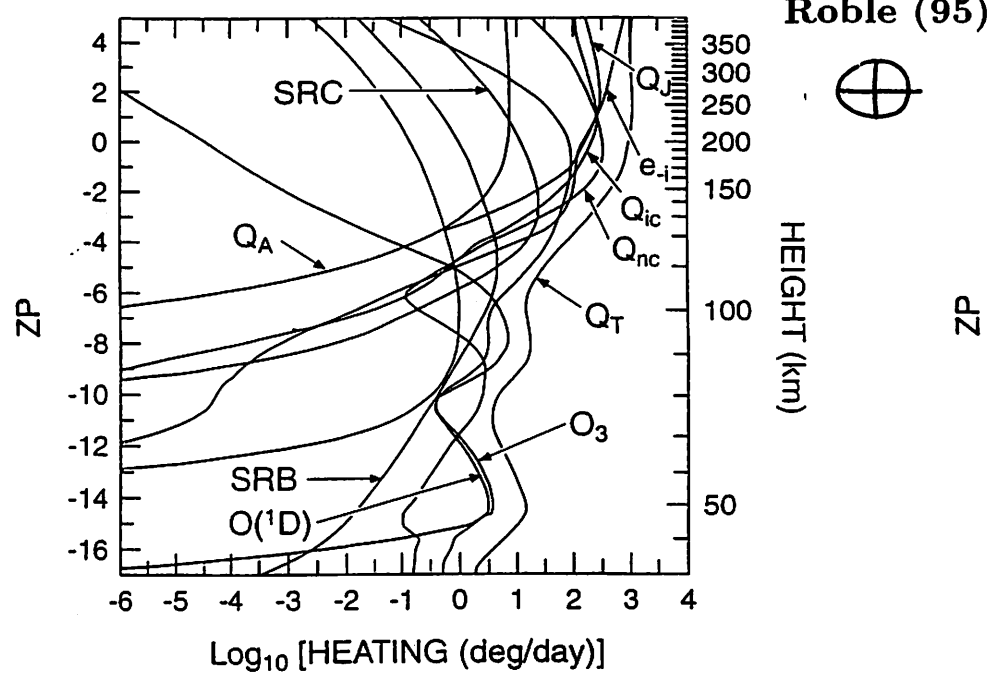


Figure 14. (Left) Heating rates due to various sources as a function of altitude for the dayside atmosphere (Fox 1988). (Right) Heating efficiencies estimated for a standard model (curve A) using a "best guess" value for the fraction of energy that appears as vibrational excitation in the quenching of metastable atomic oxygen and for a lower limit ("not unreasonable" value) model (curve B) (Fox 1988). Curve C is from Hollenbach et al. (1985). Preferred values are 16 to 25% (curves A, B) in the range of 115 to 200 km (Fox 1988).



Roble *et al.*, (87)

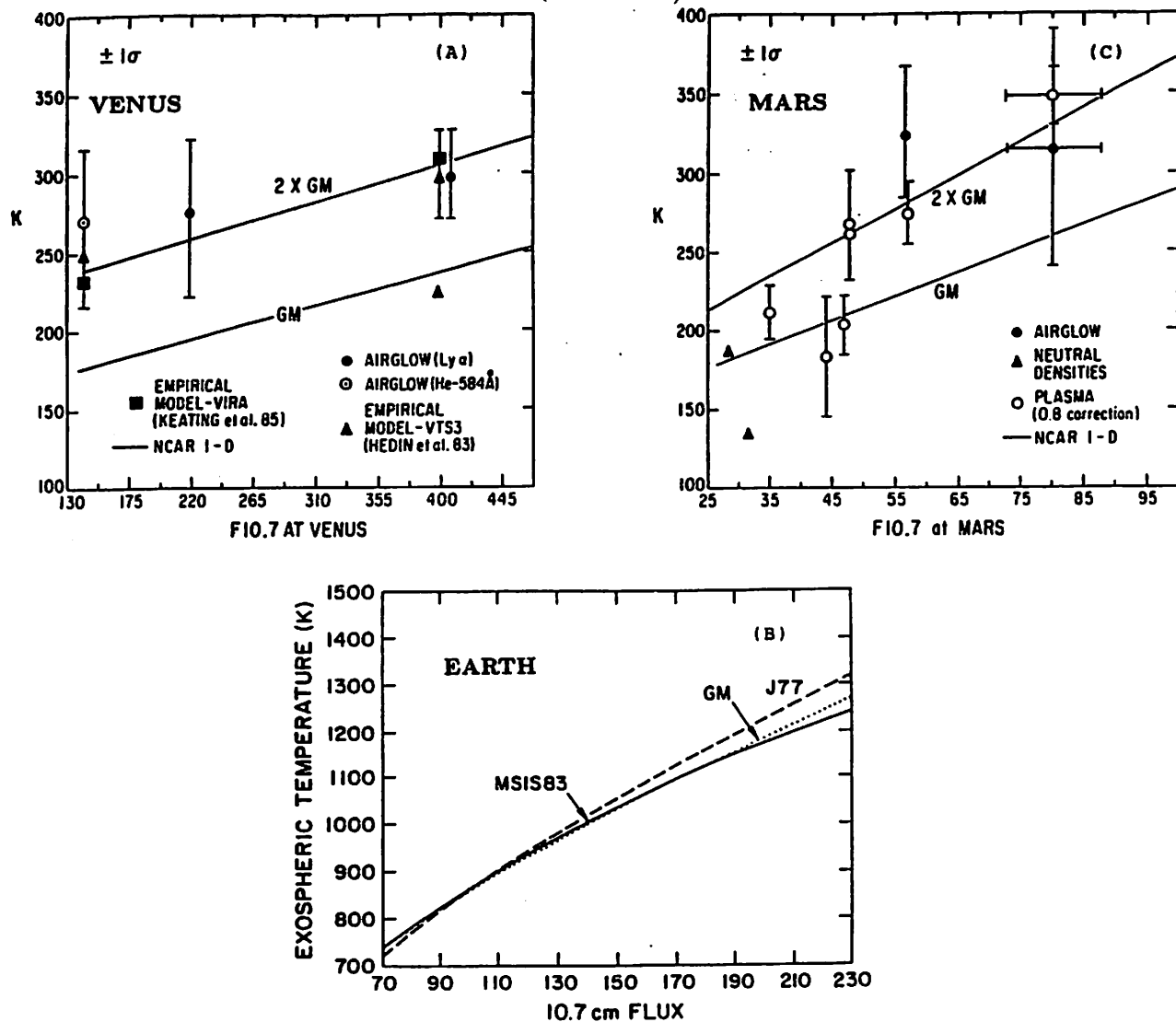


Figure 9. Global mean and dayside mean exospheric temperatures as a function of the $F_{10.7}$ -cm index scaled to each planet: (a) Venus, (b) Earth, and (c) Mars. Available data are plotted for comparison with 1-D model calculations. Dayside mean conditions are simulated with double the heating allocated to the global mean. MSIS83 refers to Hedin [1983], VIRA refers to Keating *et al.* [1985], VTS3 refers to Hedin *et al.* [1983], and J77 refers to Jacchia [1977]. Notice that the Venus solar cycle variation of global mean exospheric temperatures is far less than that observed for the Earth. The Mars variation of 150 K lies midway between that for Venus and Earth. The key lies in their respective heat budgets, specifically the relative importance of CO₂ cooling. Taken from Boughey and Rable [1991].

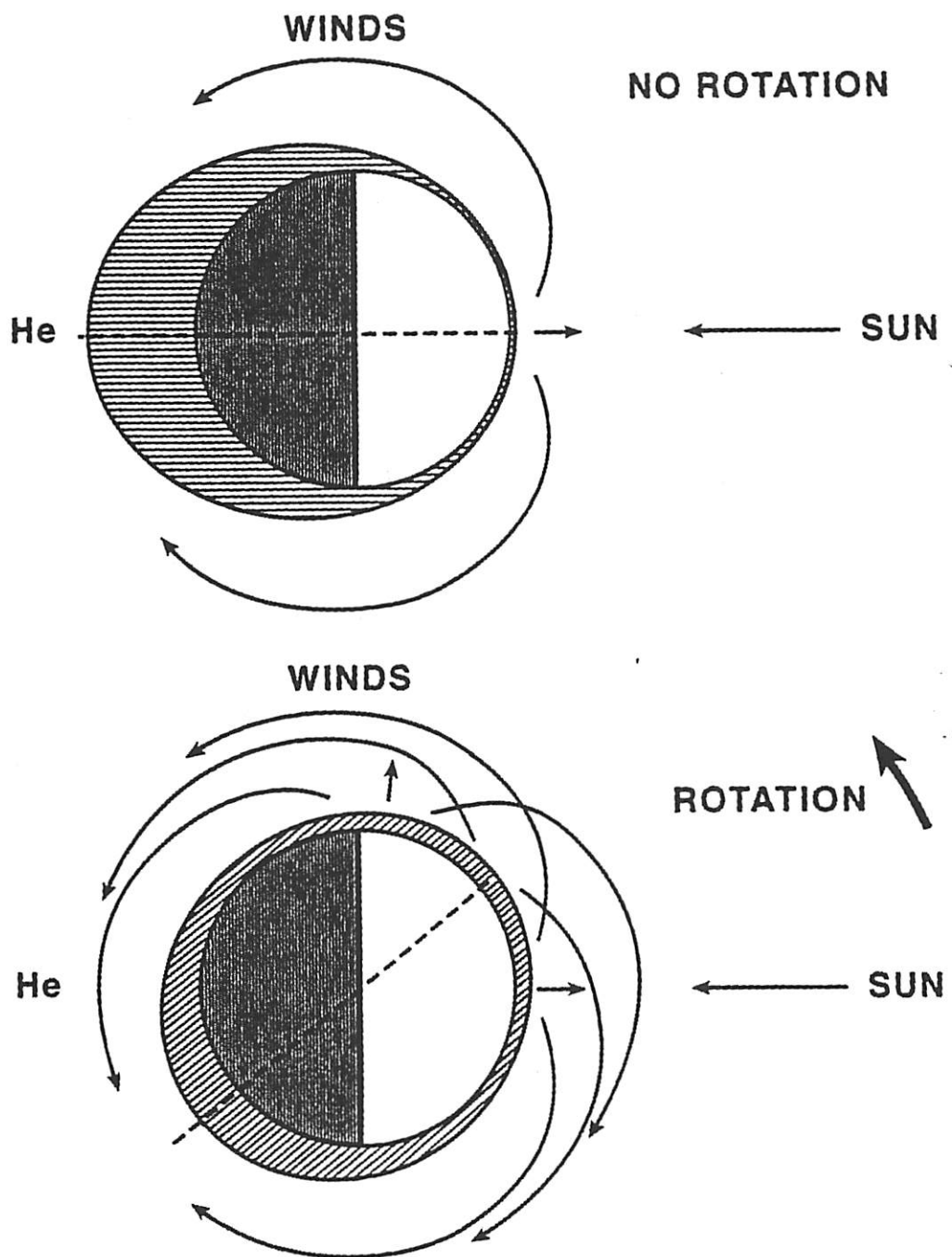
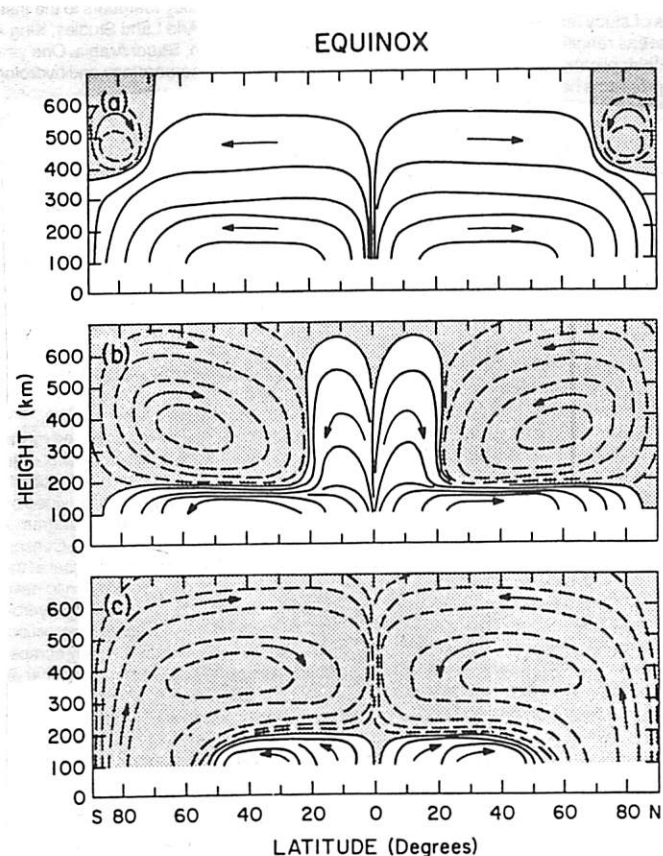


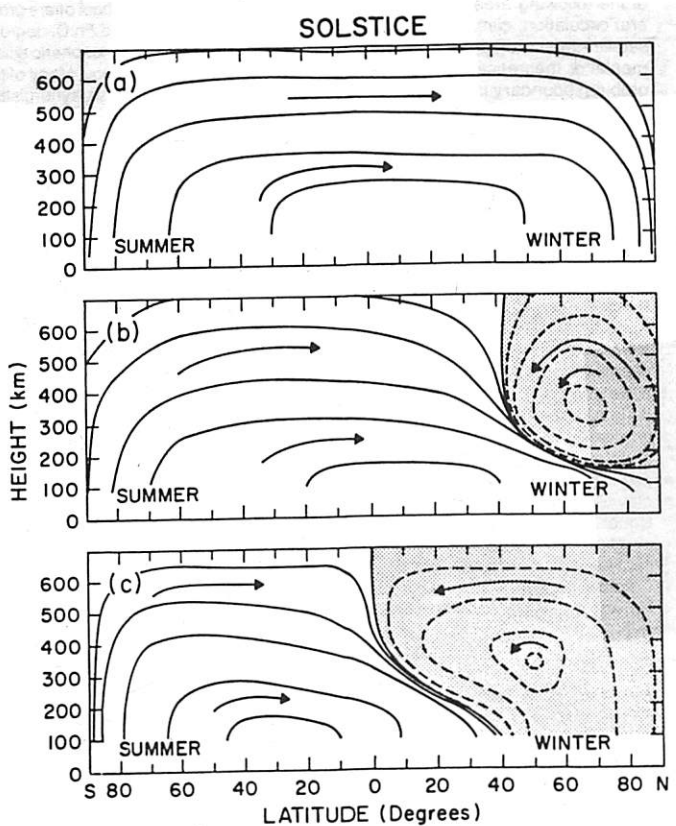
Figure 1. Cartoon of the SS-AS flow versus RSZ flow and its effects on the local time distribution of helium (figure adapted from Mayr et al. 1985).



Thermosphere Circulation Modeled



Schematic diagram of the zonal mean meridional circulation in the earth's thermosphere during equinox for various levels of auroral activity: (a) extremely quiet geomagnetic activity, (b) average activity, and (c) geomagnetic substorm. [Source: NCAR]



Schematic diagram of the zonal meridional circulation of the earth's thermosphere during solstice for various levels of auroral activity: (a) extremely quiet geomagnetic activity, (b) average activity, and (c) geomagnetic substorm. [Source: NCAR]

Kasprzak et al., (97)

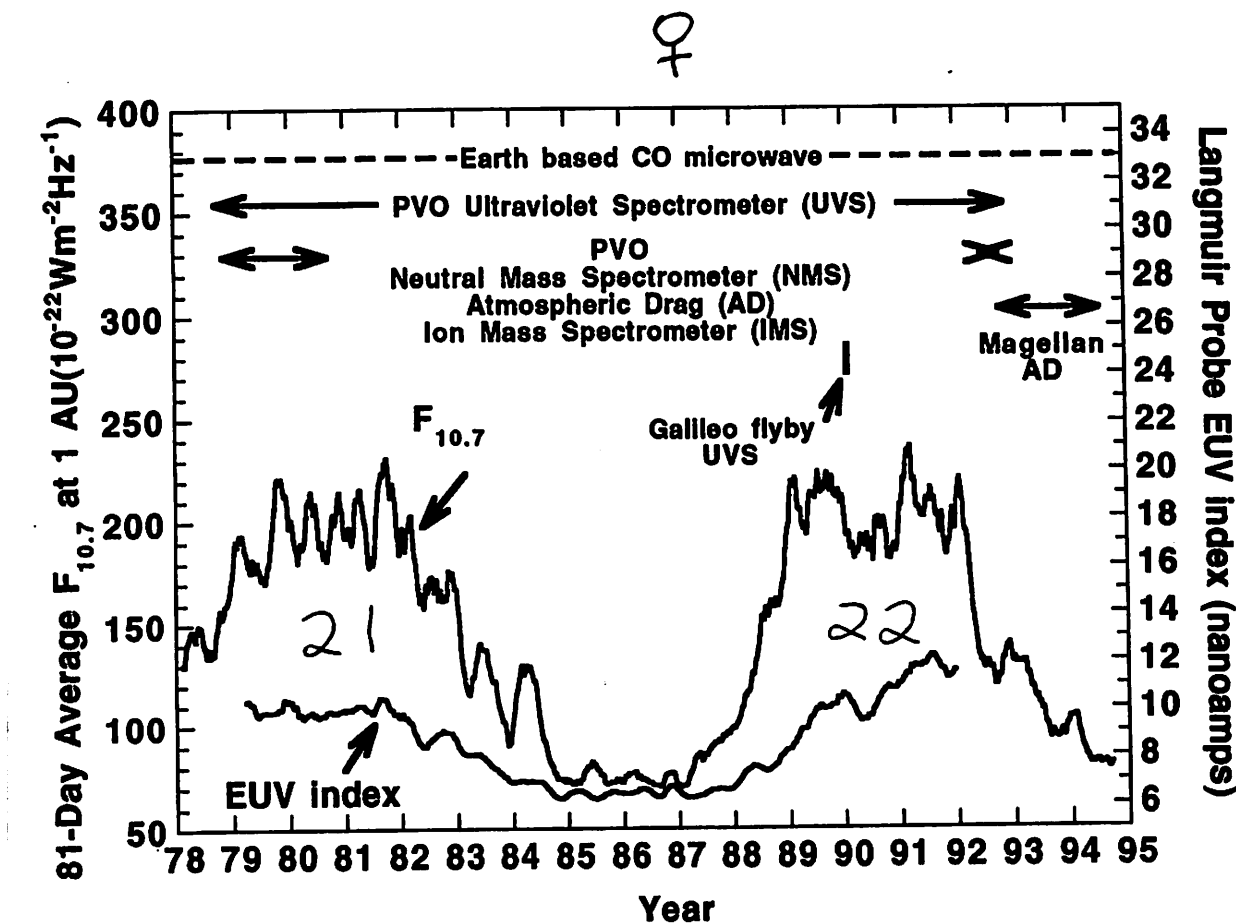


Figure 2. Solar activity as a function of year with date ranges for the various neutral density data sets obtained above 100 km. The 3-solar rotation 10.7-cm radio flux index, $F_{10.7}$, is measured at Earth and adjusted for the difference in phase of Earth and Venus. The solar EUV index, I_{pe} (Brace et al. 1988) is measured at Venus and has more than half of its contribution from Lyman- α .

Kasprzak *et al.*, (97)

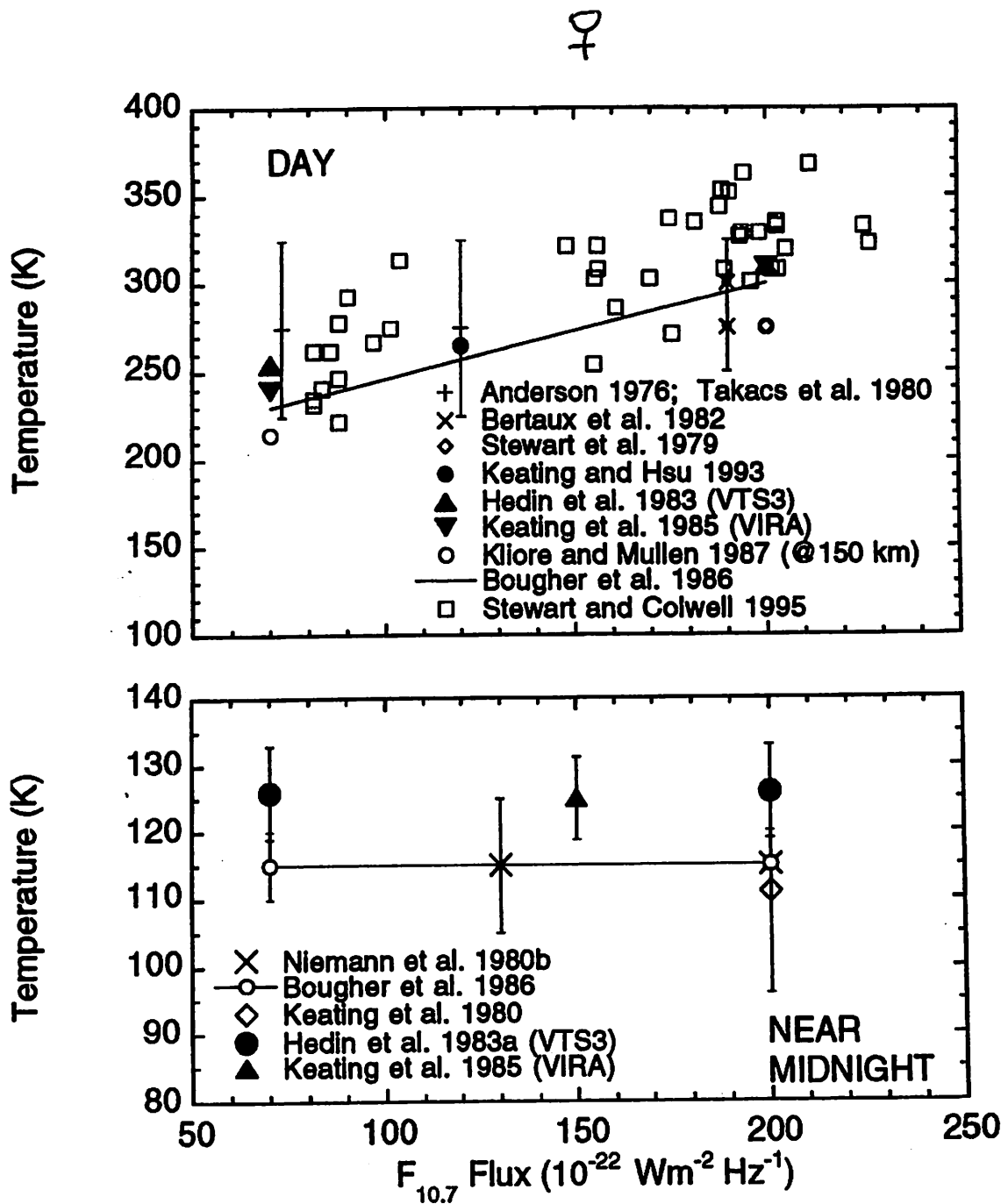


Figure 12. Dayside and near midnight exospheric temperatures measured over the solar cycle and predicted by several models for Venus.

10

SOLAR ACTIVITY BEHAVIOR OF THE THERMOSPHERE

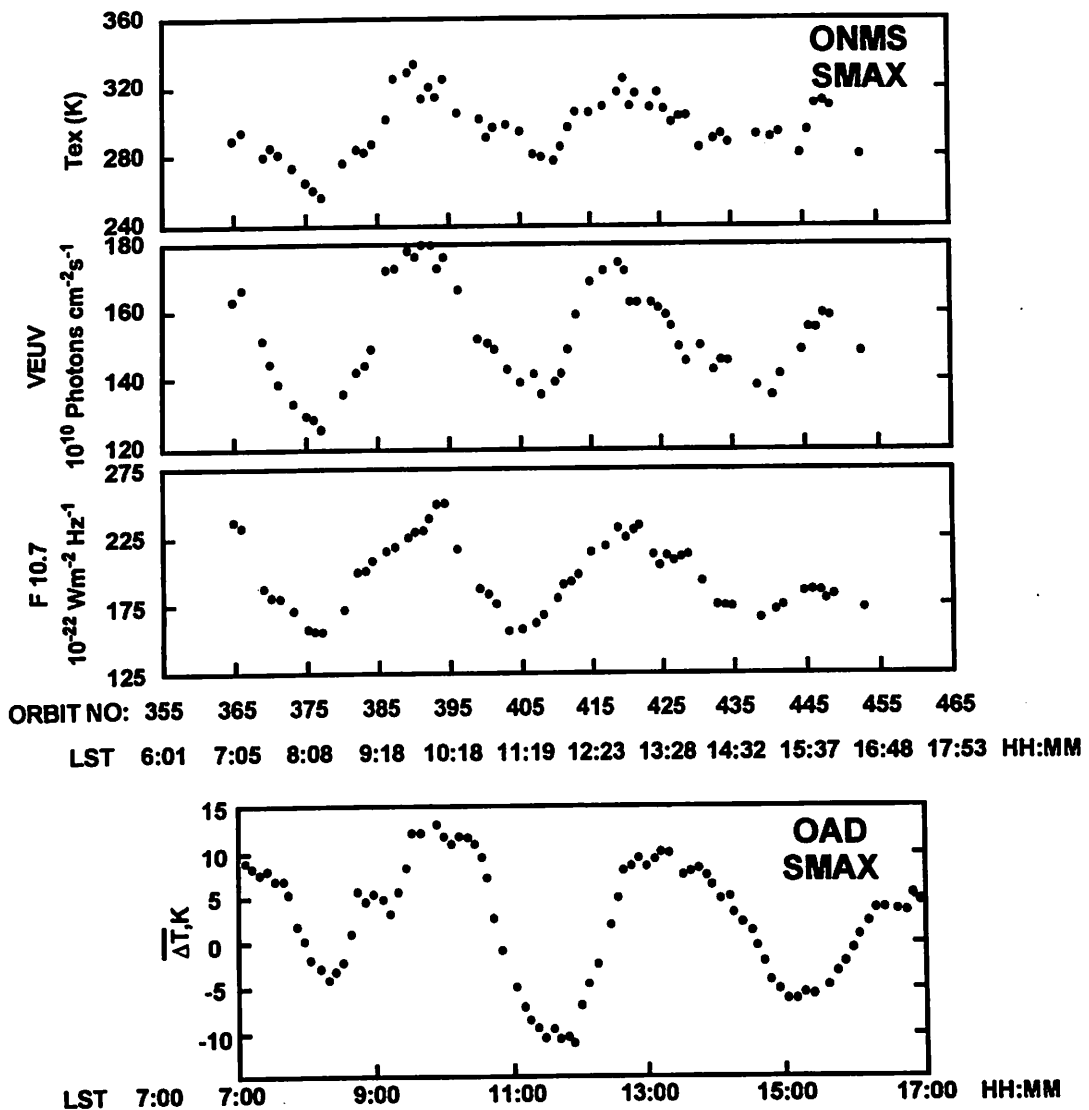
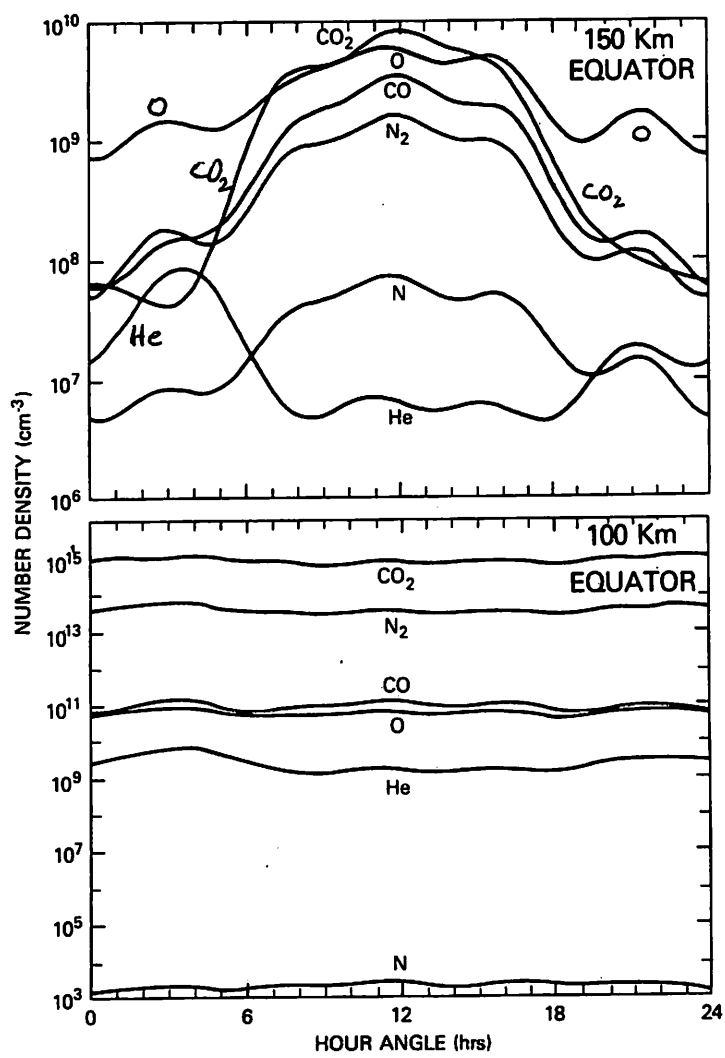
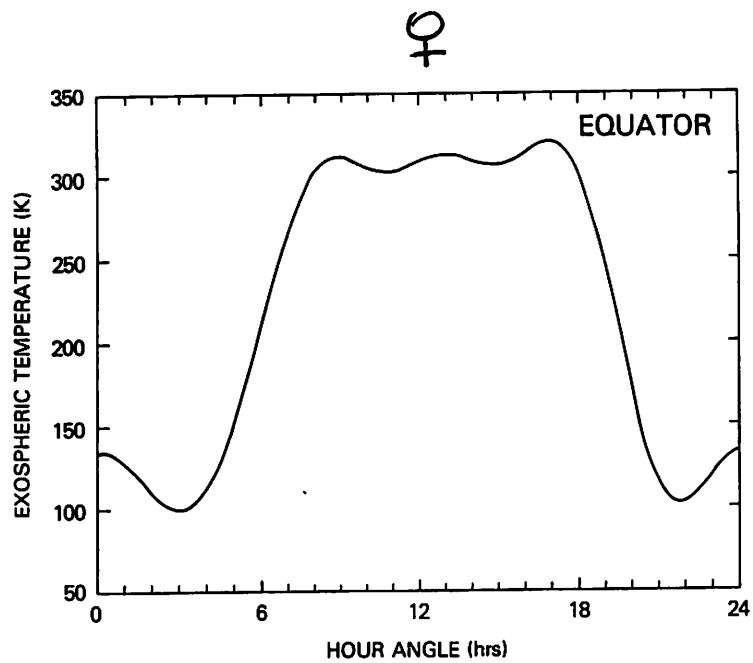


Figure 7. Scale-height temperatures, Tex, derived from PV ONMS dayside atomic oxygen measurements (Niemann *et al.* 1980*b*), the Langmuir Probe VEU index (Brace *et al.* 1988), the daily $F_{10.7}$ index (corrected for the Earth-Venus phase difference) (Mahajan *et al.* 1990) and PV OAD exosphere temperature change derived from mass density measurements (Keating and Bougher 1992*a,b*) plotted as a function of local solar time.

Hedin *et al.*, (83) VTS3

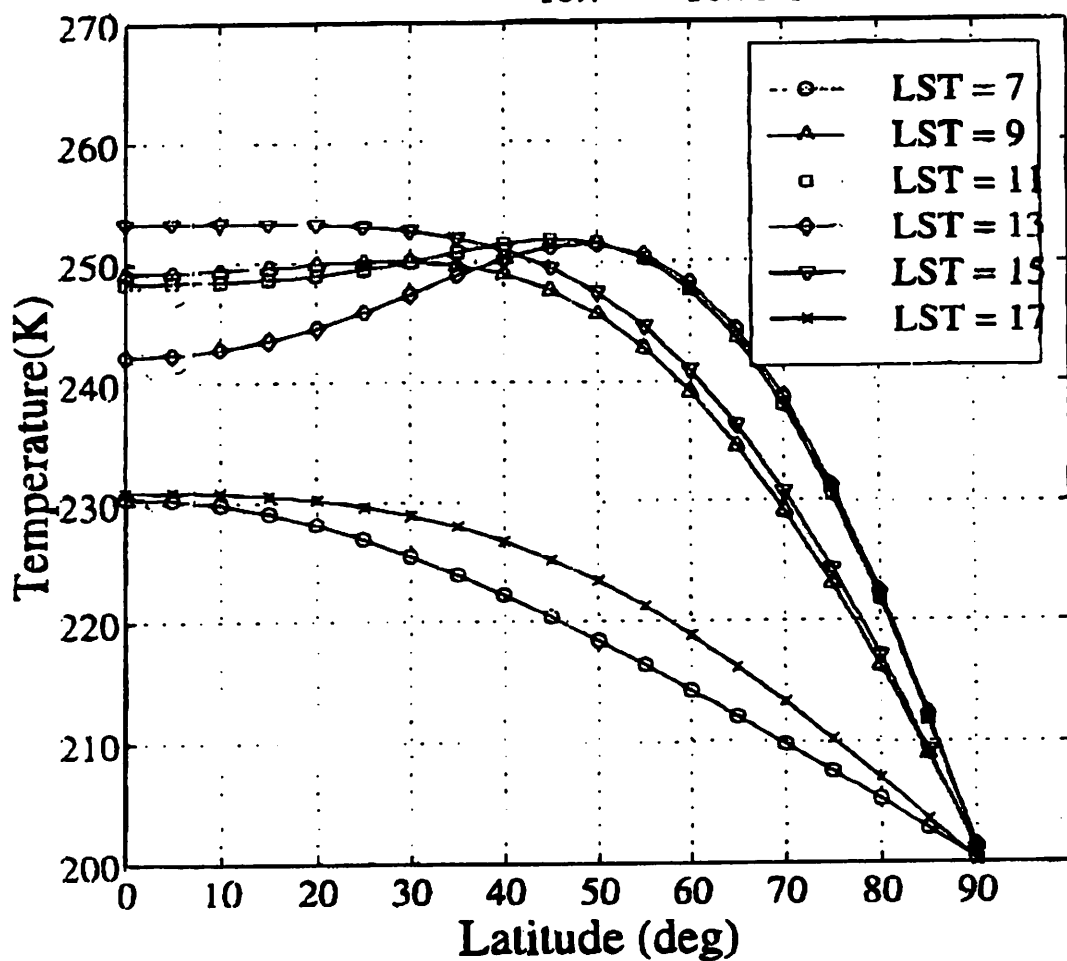


Keating *et al.*, (98) VIRA98

O
+

VIRA 98 Temperature vs Latitude

Alt = 165 ; $F_{10.7} = F_{10.7\text{bar}} = 80$



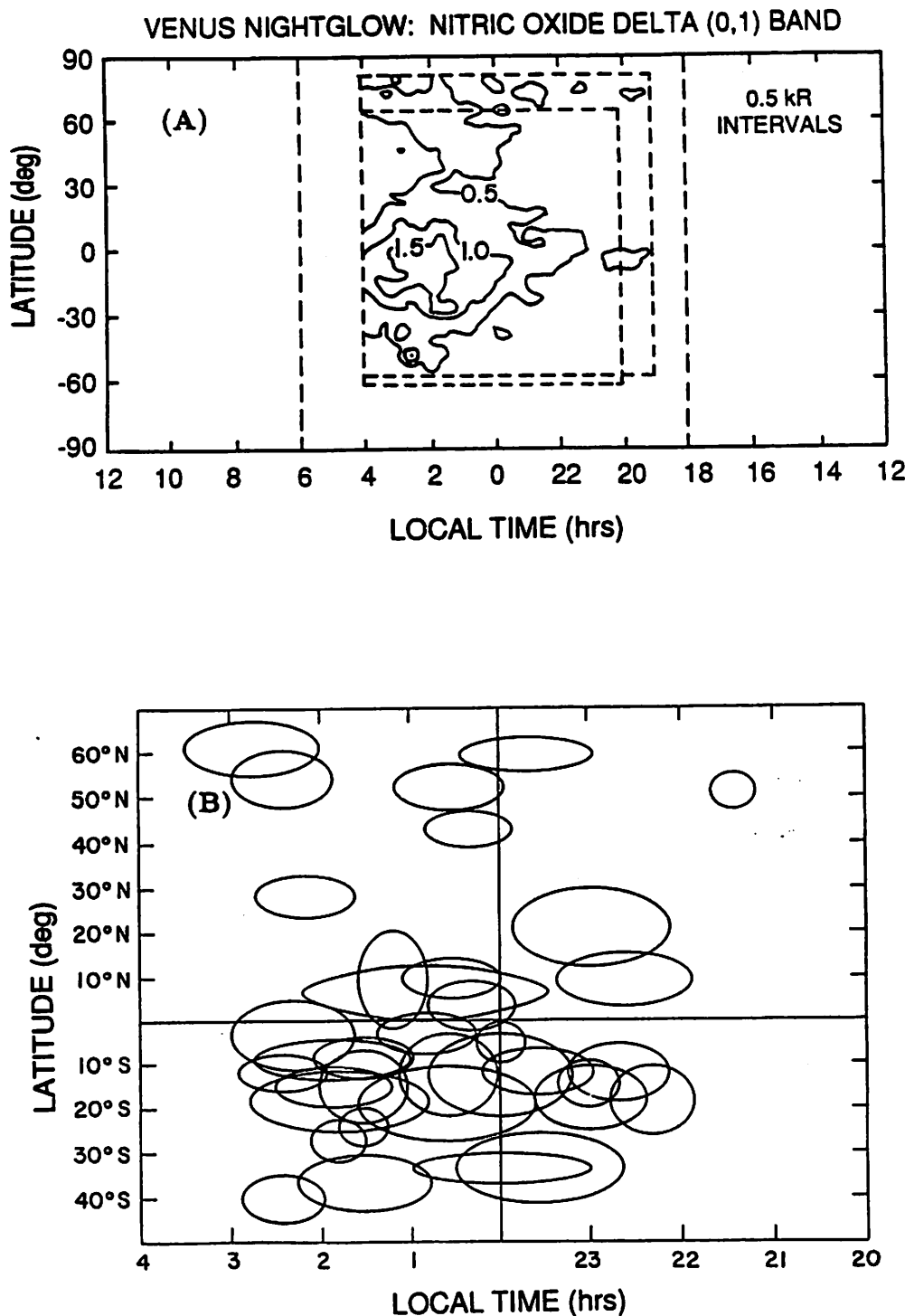
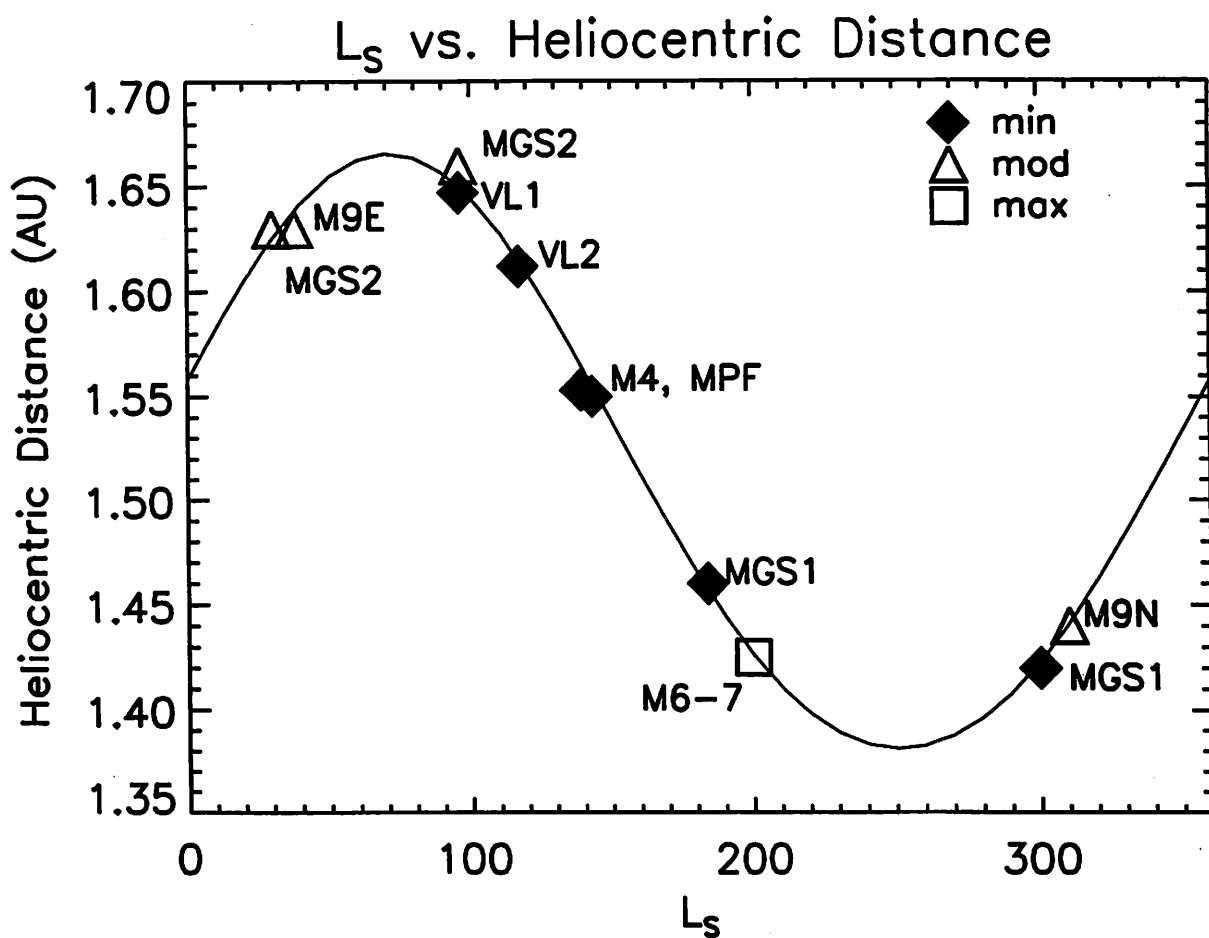


Figure 2. (a) The OUVS NO(0,1) δ -band vertical intensity distribution. The latitude and local time grid is filled with 198 nm data as obtained and revised in absolute intensity according to Bougher *et al.* (1990). This statistical map of the airglow is obtained over 35 orbits early in the PVO mission, and exhibits a dark-disk average intensity (120–180° SZA) of $460 \pm 120 R$. (b) Spatial variability of the observed OUVS 198 nm individual bright airglow patches included in the statistical map of (a). The half maximum intensity spatial extent of each individual NO patch is plotted as a function of local time and latitude. The aspect ratio, defined as the local time to latitude ratio, of each equatorial to mid-latitude patch is on the order of 2:1. This value is largely independent of latitude, and it implies strong zonal winds (figure from Bougher *et al.* 1990).

Bouguer *et al.*, (00)

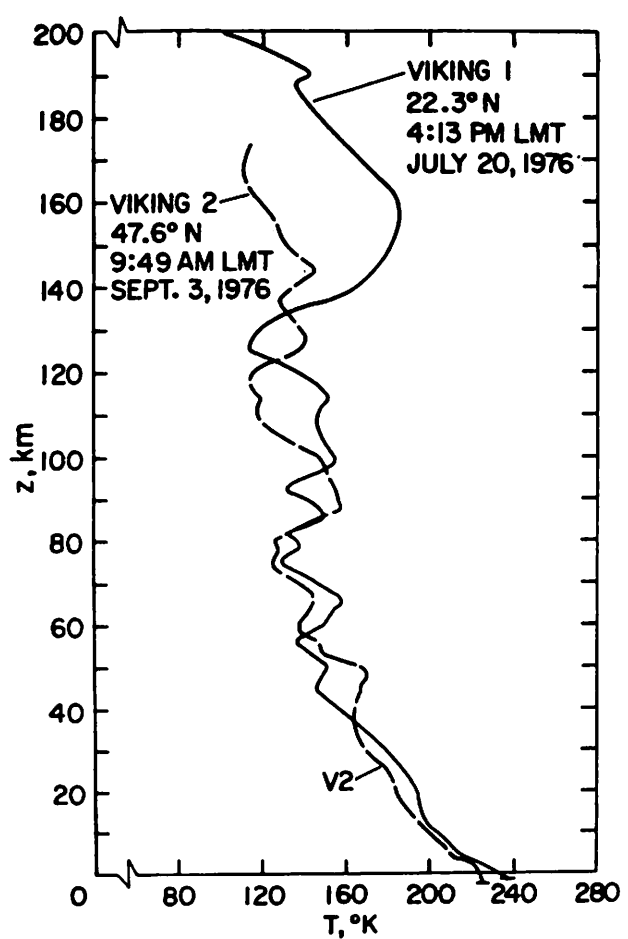


Bougher et al. (2000)

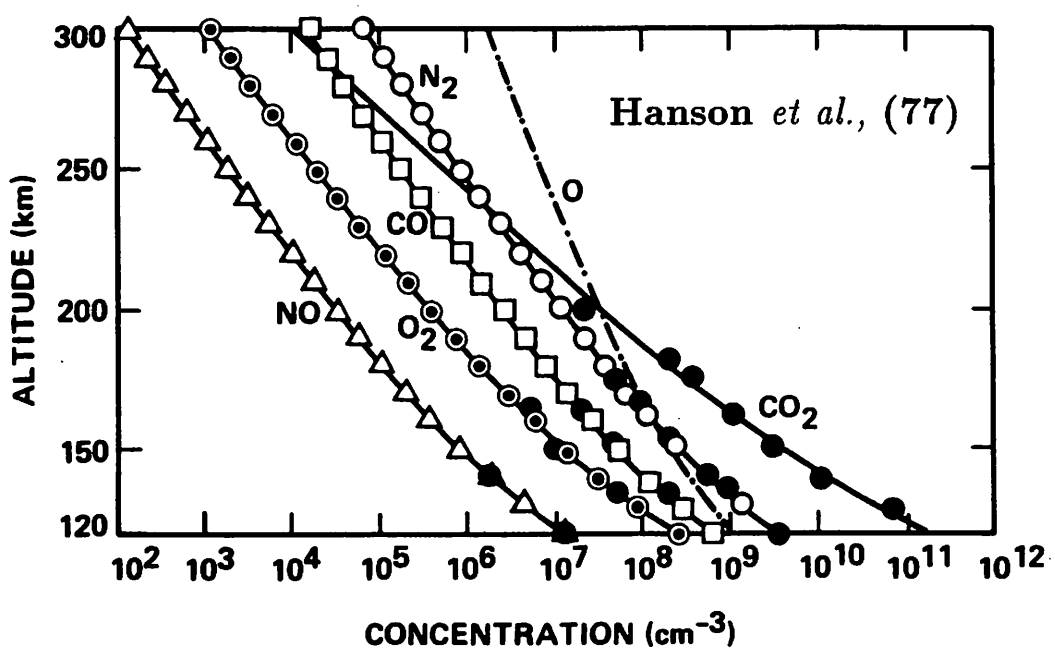
Table 1. Mars Spacecraft Observations of the Upper Atmosphere

Spacecraft	Dates(s)	F10.7	Ls	Dsm	SZA	Texo
M4	650715	77.0	139.0	1.553	67.0	212.0
M67	690731	167.0	200.0	1.425	57.0	315-350.0
	690805	188.0				
M9N	71FALL	103.0	306.0	1.440	50-60.0	325.0
M9E	72SPRG	100.0	38.0	1.630	70-90.0	268.0
VL1	760720	69.0	96.0	1.647	44.0	186.0
VL2	760903	76.0	117.0	1.612	44.0	145.0
MPF	970704	70.0	143.0	1.557	135.0	153.0
MGS1	980116	93.0	256.0	1.382	73.5	220.0
MGS2	981027	127.0	48.5	1.653	57.0	230.0

F10.7 refers to the 10.7-cm index used to select reference EUV/UV flux datasets; Ls refers to the angular measure of the Mars seasons (Ls = 90 is Northern Summer Solstice, Ls = 270 is Southern Summer Solstice, etc.); Dsm refers to the Mars heliocentric distance (AU); SZA refers to solar zenith angle; T-exo refers to exospheric temperature. Dates are listed as follows: YYMMDD. Spacecraft are indicated as follows; M4 (Mariner 4), M67 (Mariner 6 and 7), M9E (Mariner 9 Extended), M9N (Mariner 9 Nominal), VL1 (Viking Lander 1), VL2 (Viking Lander 2), MPF (Mars Pathfinder), MGS1 (Mars Global Surveyor Phase 1 Aerobraking sample), MGS2 (Mars Global Surveyor Phase 2 Aerobraking sample).

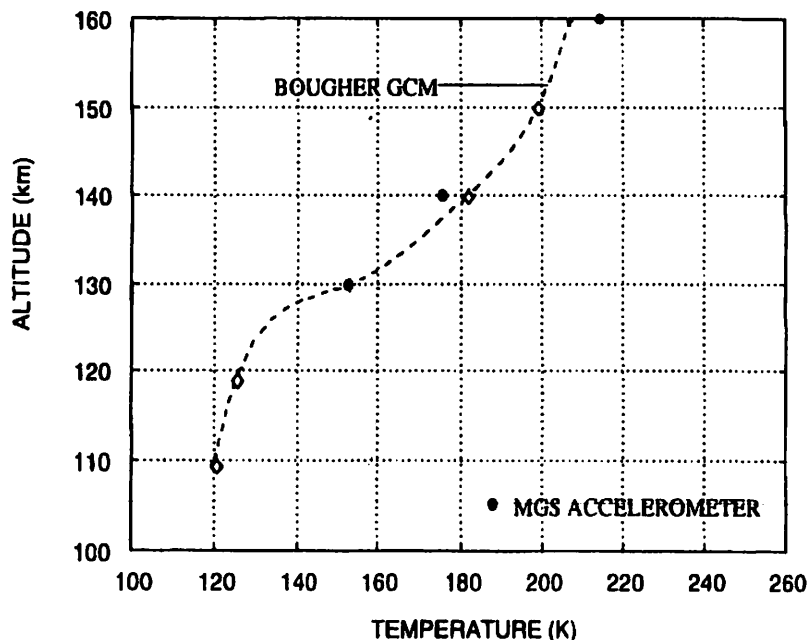


Seiff and Kirk (77)



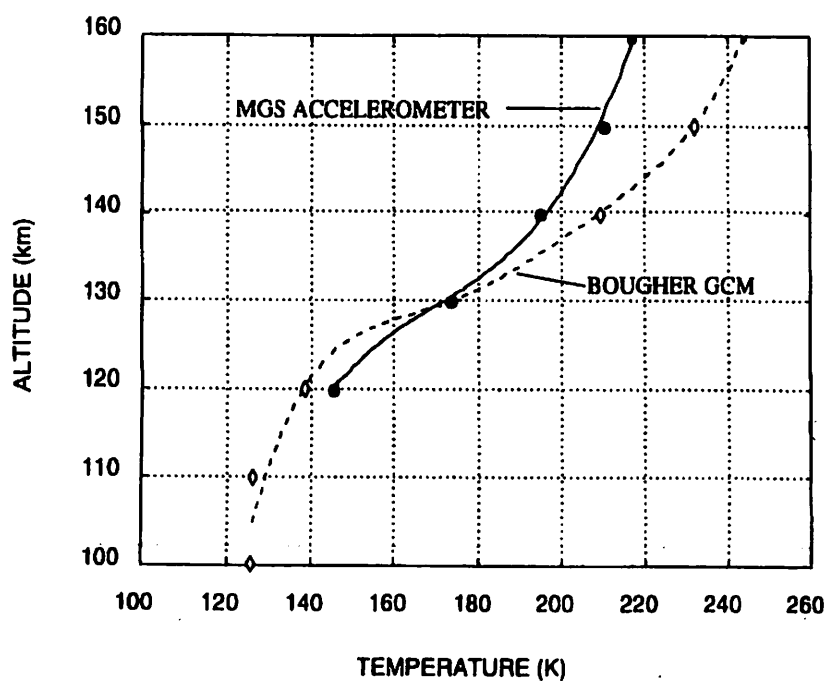
Bouger and Keating (99)

MARS THERMOSPHERIC TEMPERATURE STRUCTURE 45N FALL/WINTER LOW SOLAR ACTIVITY



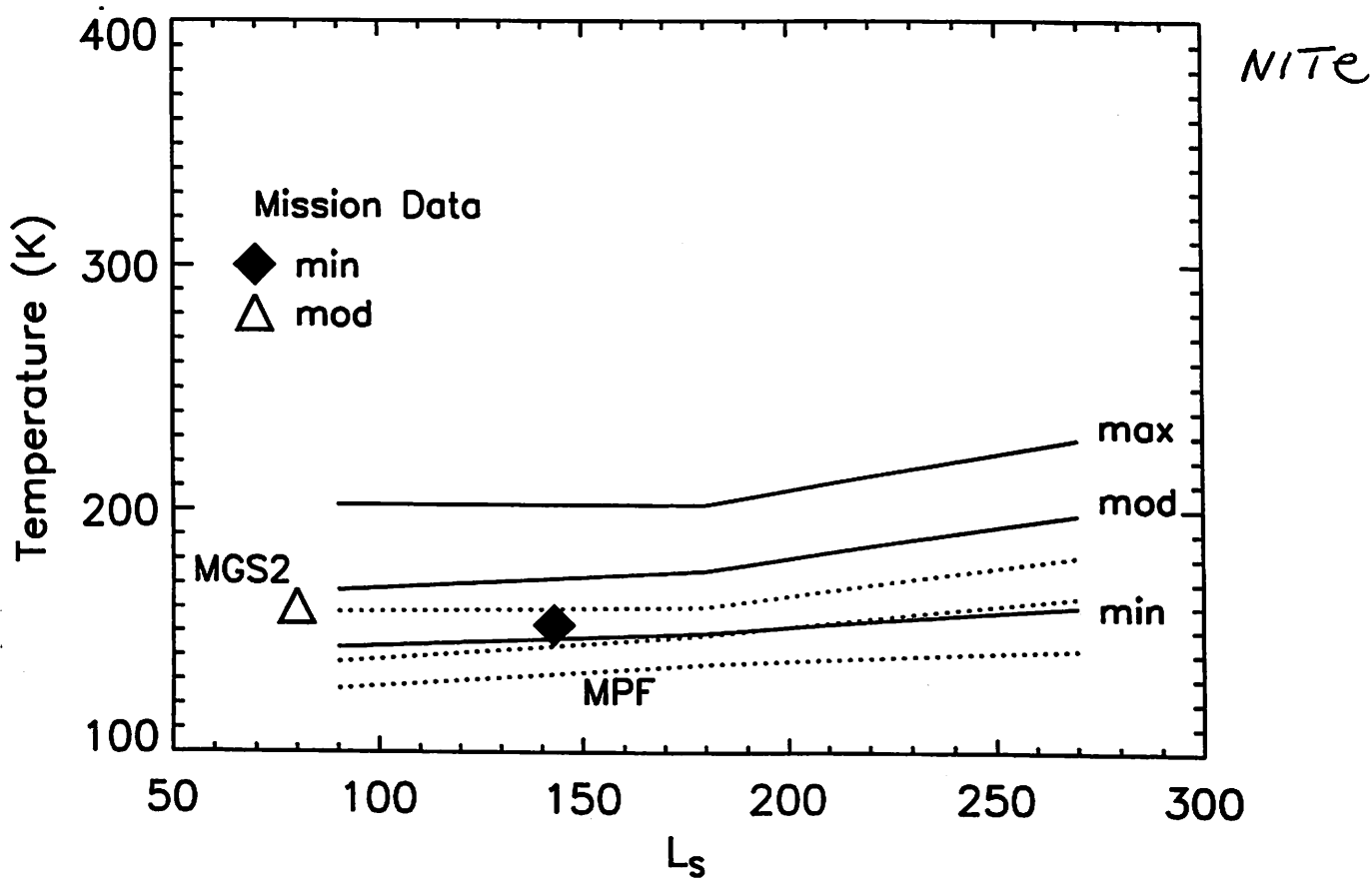
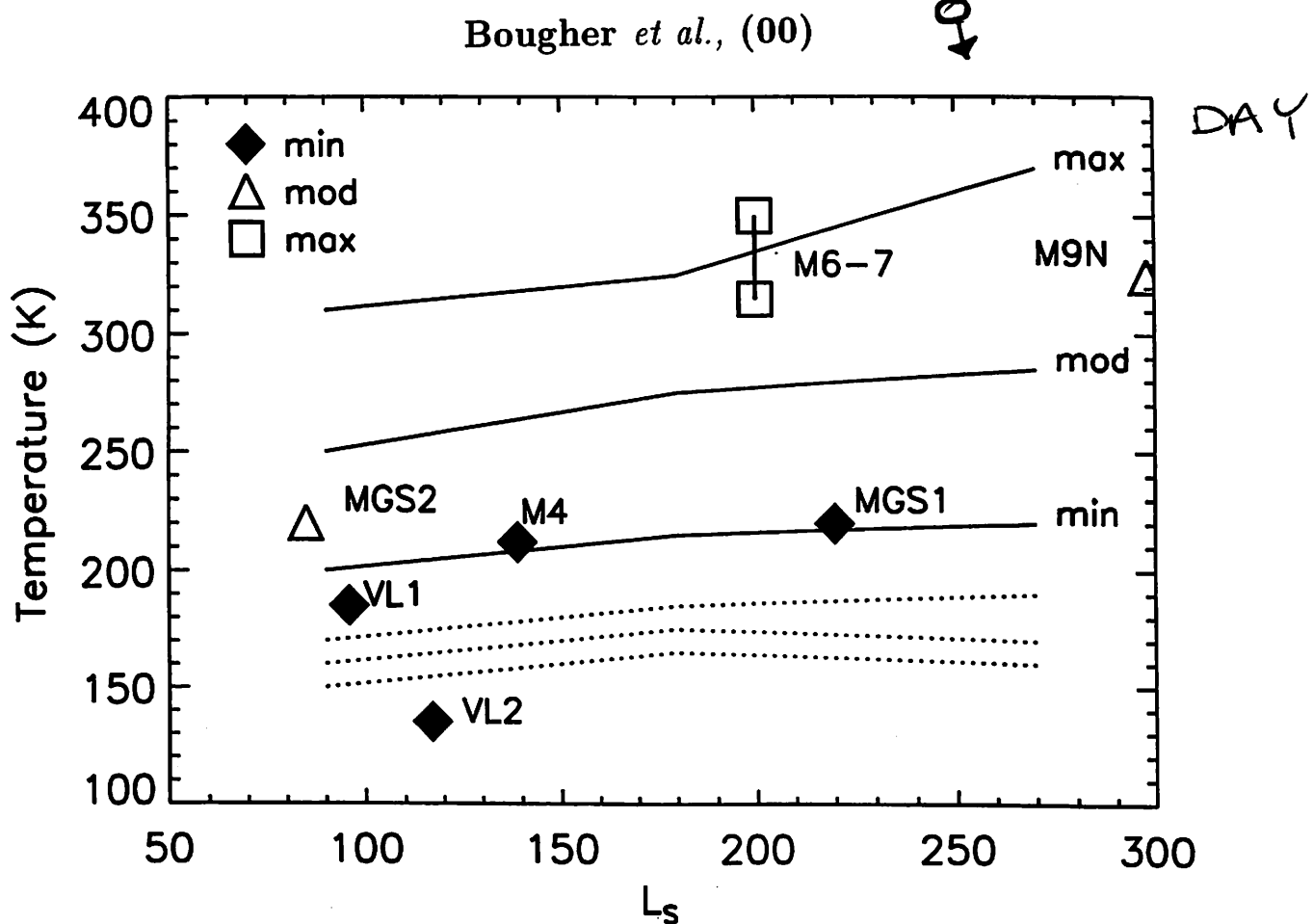
PHASE I
AB

MARS THERMOSPHERIC TEMPERATURE STRUCTURE 45N SPRING/SUMMER MEDIUM SOLAR ACTIVITY



PHASE II
AB

Bougger *et al.*, (00)



Bougher et al. (2000)

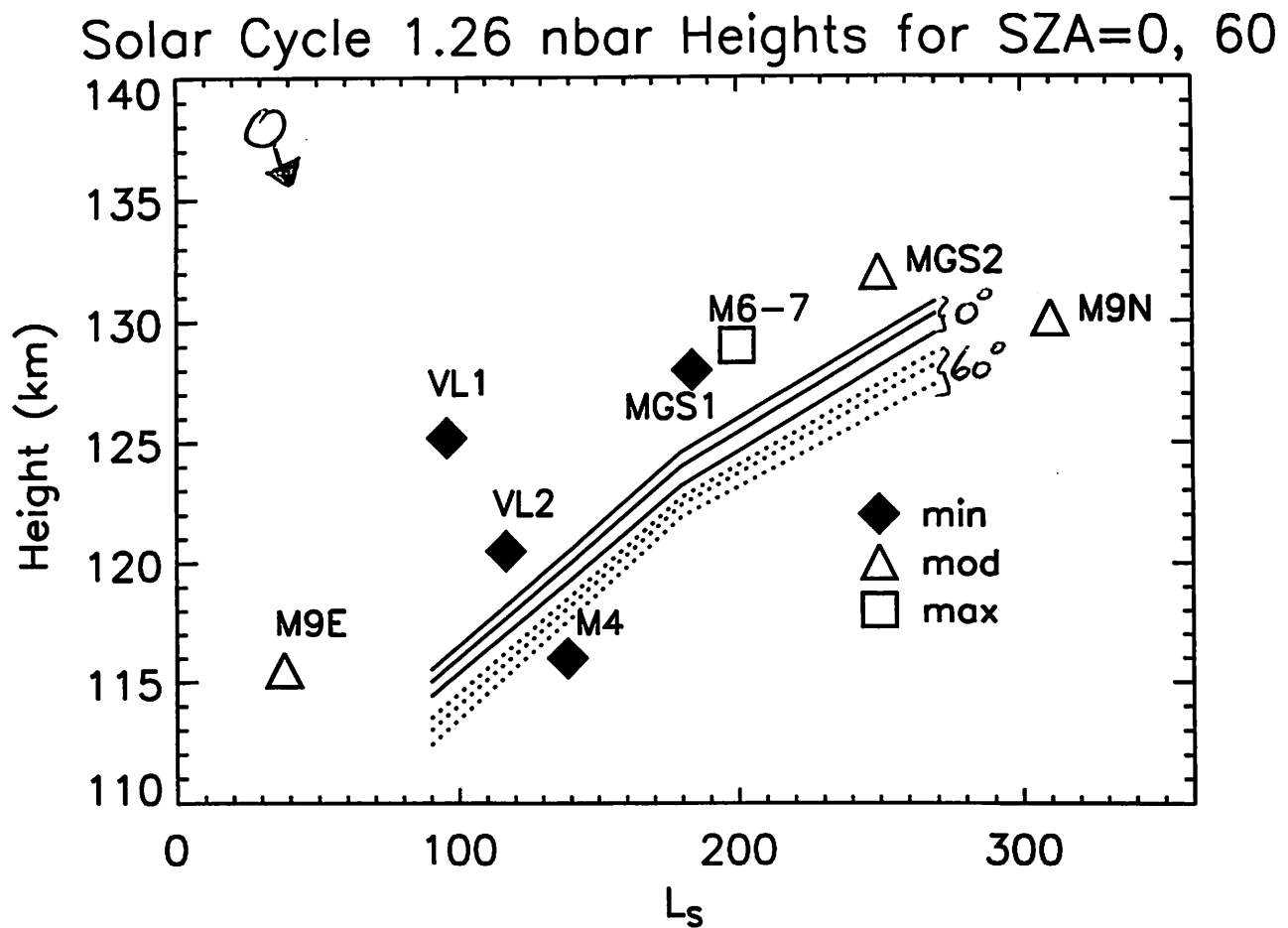
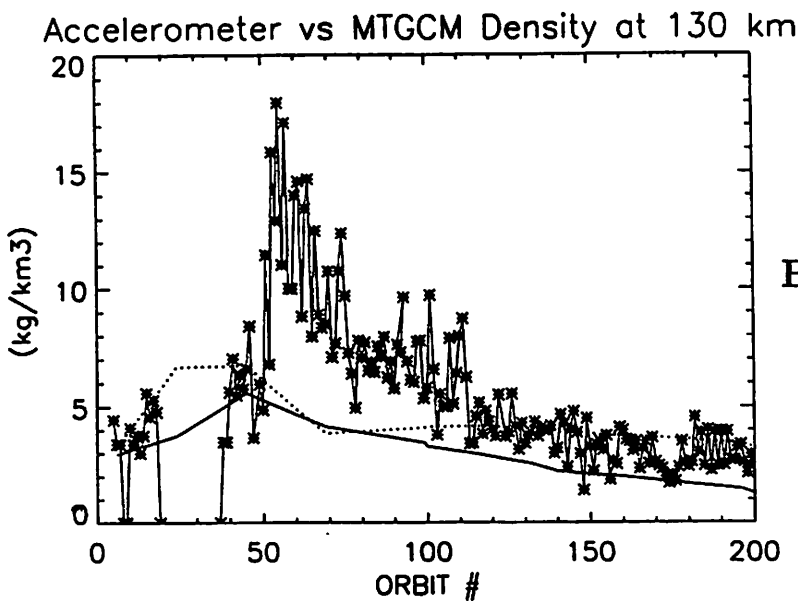


fig 6



Bouger et al., (99a)

Fig. 2 MGS Accelerometer versus MTGCM simulated mass densities at 130 km for P050-P200. A combination of latitude, local time, longitude and dust variations encountered at the spacecraft periapses is contained in the MGS Accelerometer densities. MTGCM simulations account for latitude, local time, and dust variations. MGS data (asterisks), MTGCM simulations for static $\tau = 0.3$ dust case (solid line), and MTGCM simulations for static $\tau = 1.0$ dust case (dotted line).

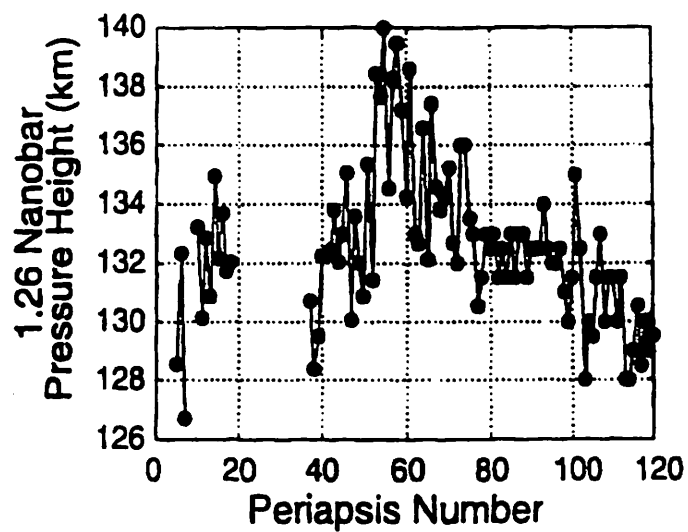
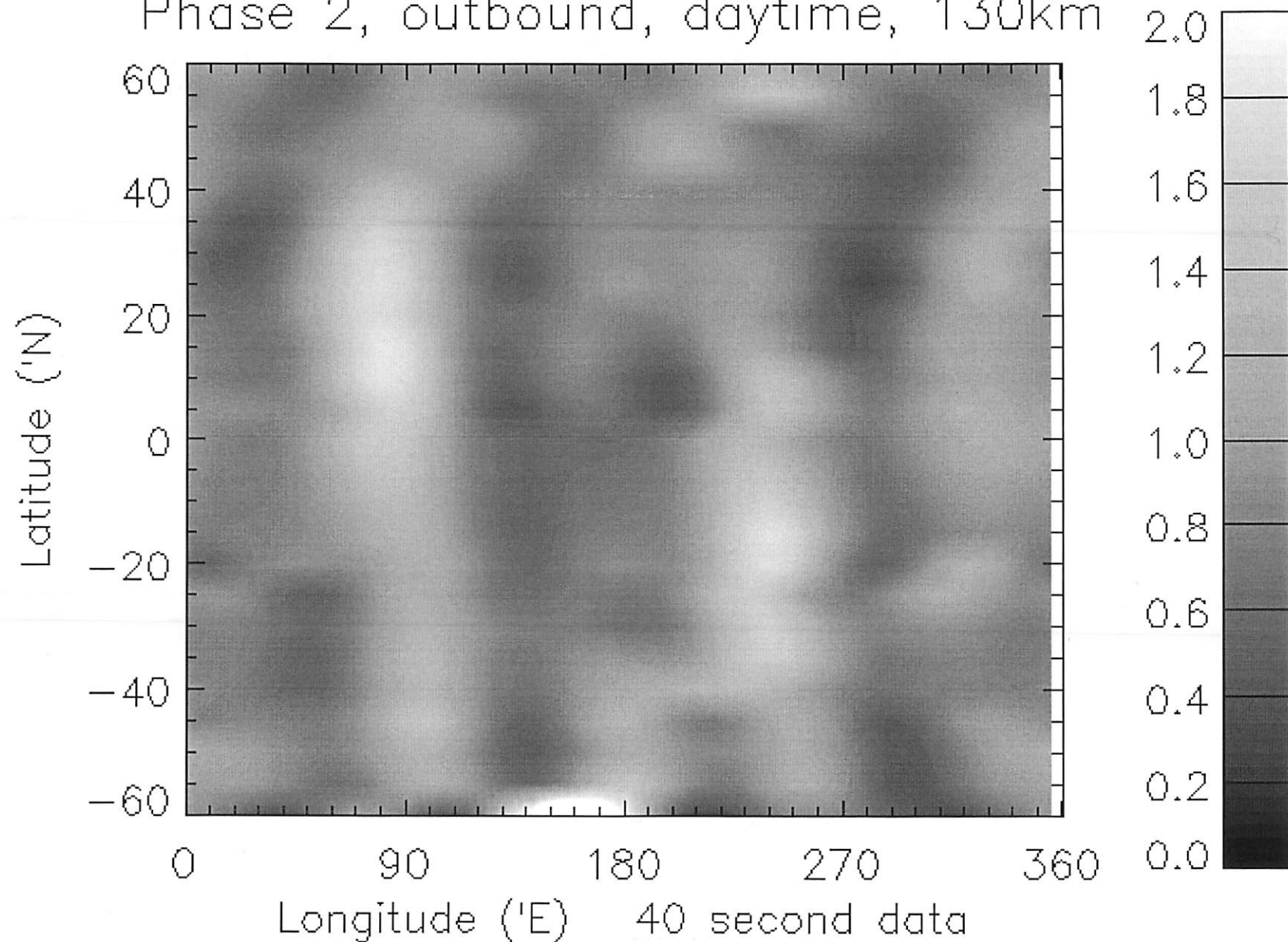


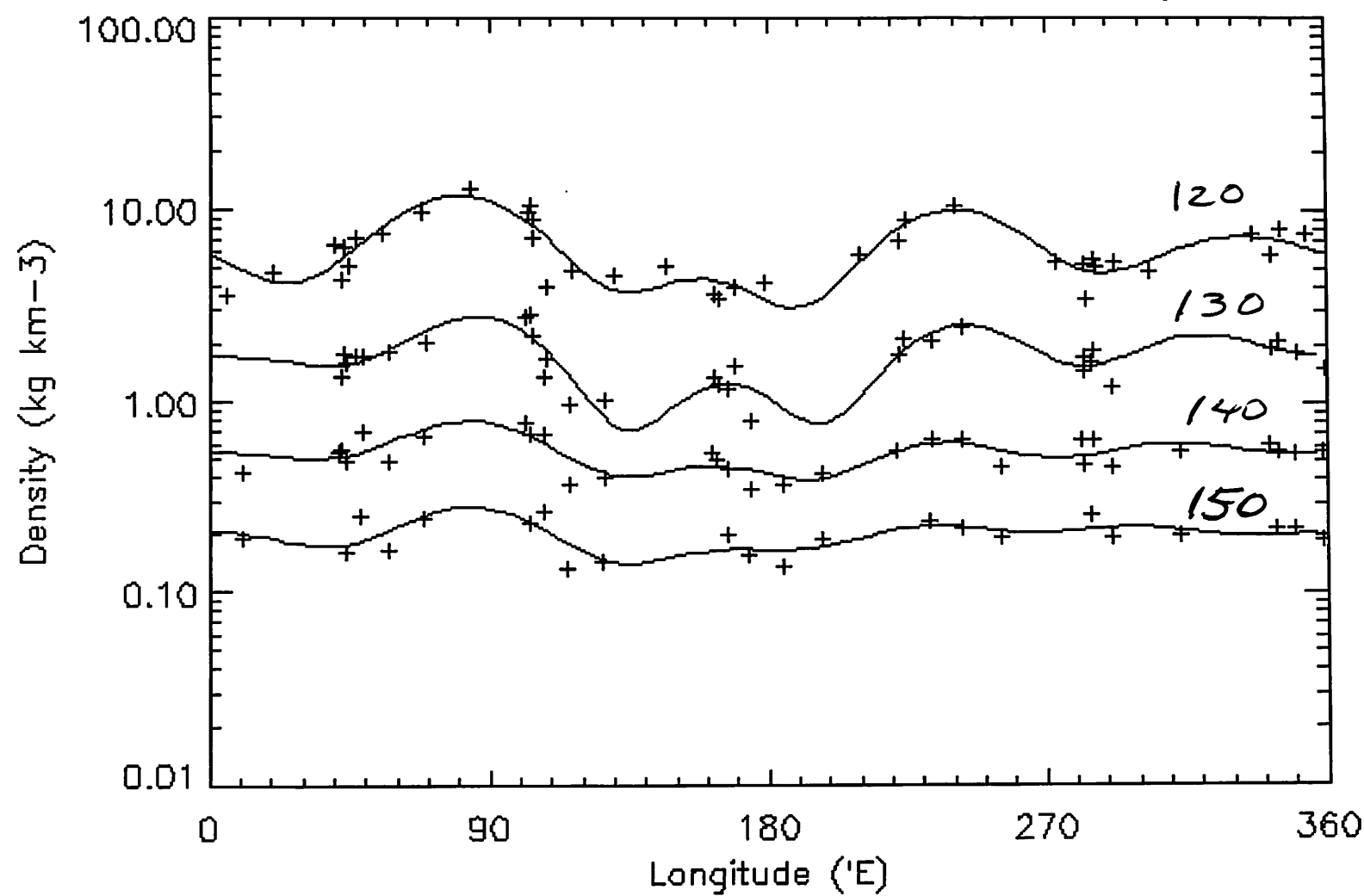
Fig. 3 MGS Accelerometer 1.26-nanobar pressure heights measured during Phase I aerobraking (P005-P120). Taken from Keating et al. (1998).

Fitted density ratioed to mean fitted density
Phase 2, outbound, daytime, 130km



MGS

Wave-5 fit to outbound densities
Phase 2, 0 to 10 °N, 40 second data, daytime



+ = MGS data, solid line = least squares wave-5 fit,
dotted lines = 1 sigma uncertainty in fit,
levels = 120 130 140 150 km

VTGCM AND MTGCM THERMOSPHERE MODELS : BASIC DESCRIPTIONS

- VTGCM : NCAR Venus Thermospheric GCM (94-200 km)

- Resolution : $5 \times 5^\circ$ horizontal; 32-layers
- Neutral Fields : T, U, V, W, O, CO, CO₂, N₂, O₂, He
- Odd Nitrogen Fields : NO, N(⁴S), N(²D)
- Airglow Fields : NO(198.0 nm), O₂(1.27-micron and 400-800 nm)
- Ion Fields : PCE Only (O₂⁺, CO₂⁺, O⁺, NO⁺)
- Ion-neutral reactions and rates from Massie *et al.*, [1983]
- Prescribed EUV (20%) and UV (22%) heating efficiencies.
- Eddy diffusion coefficient : $\leq 1.0 \times 10^7 \text{ cm}^2/\text{sec}$
- Gravity wave drag : slowing day-to-night wind speeds by factor of 2

- MTGCM : NCAR Mars Thermospheric GCM (70-300 km)

- Resolution : $5 \times 5^\circ$ horizontal; 32-layers
- Neutral Fields : T, U, V, W, O, CO, CO₂, N₂, O₂, AR
- Ions : PCE (O₂⁺, CO₂⁺, O⁺, NO⁺, CO⁺, N₂⁺ $\leq 200 \text{ km}$)
- Ions : DYN (O₂⁺, O⁺ $\geq 200 \text{ km}$)
- Ion-neutral reactions and rates from Fox *et al.*, [1995]
- Empirical electron and ion temperatures from Fox [1993]
- Prescribed EUV/UV (22%) heating efficiencies.
- Eddy diffusion coefficient : $\leq 1.0-3.0 \times 10^7 \text{ cm}^2/\text{sec}$
- Non-Solar Forcing : semi-diurnal tides

Coupling of Mars Lower and Upper Atmospheres

- Mars fundamental parameters for season from AMES MGCM (0-90 km)
- Zonally and time averaged Ts and heights exchanged at p=1.32-ubar
- Semi-diurnal tidal amplitudes and phases exchanged at p=1.32-ubar

Dusty Lower Atmosphere Cases

- Static dust, globally horz. uniform with specified vertical distribution
- tau (visible) = 0.3 to 1.0, spanning MGS aerobraking data outside storm
- Inflation accommodated by MGCM zonally averaged heights
- Waves accommodated by MGCM semi-diurnal tidal fields

TIEGCM MODEL

(THERMOSPHERE-IONOSPHERE-ELECTRODYNAMICS) :

BASIC DESCRIPTION

A. Calculation Scheme/Solution System

- Independent Variables : z, λ (long.), ϕ (lat.), t (time)
- Many Prognostic Equations : T, U, V, 9-SPECIES
- Major Neutral Species = O, O₂, N₂
- Minor Neutral Species = N(²D), N(⁴S), NO, He, Ar
- Plasma Species = O⁺, O₂⁺, NO⁺, N₂⁺, N⁺, electrons
- Plasma Temperatures = Tion, Telec
- Two Diagnostic Equations : W, Φ
- Dynamo electric field and currents

B. Geometry/Model Resolution

- Vertical : $z = \log(p_0/p)$: $p_0 = 0.5\text{-nbar}$; $\Delta z=0.5$ Levels (29) ; Thermos-Ionos.: -7 to 7 or 95-800 km
- Horizontal : 5 x 5° Grid; 0-24 LT; Pole to pole

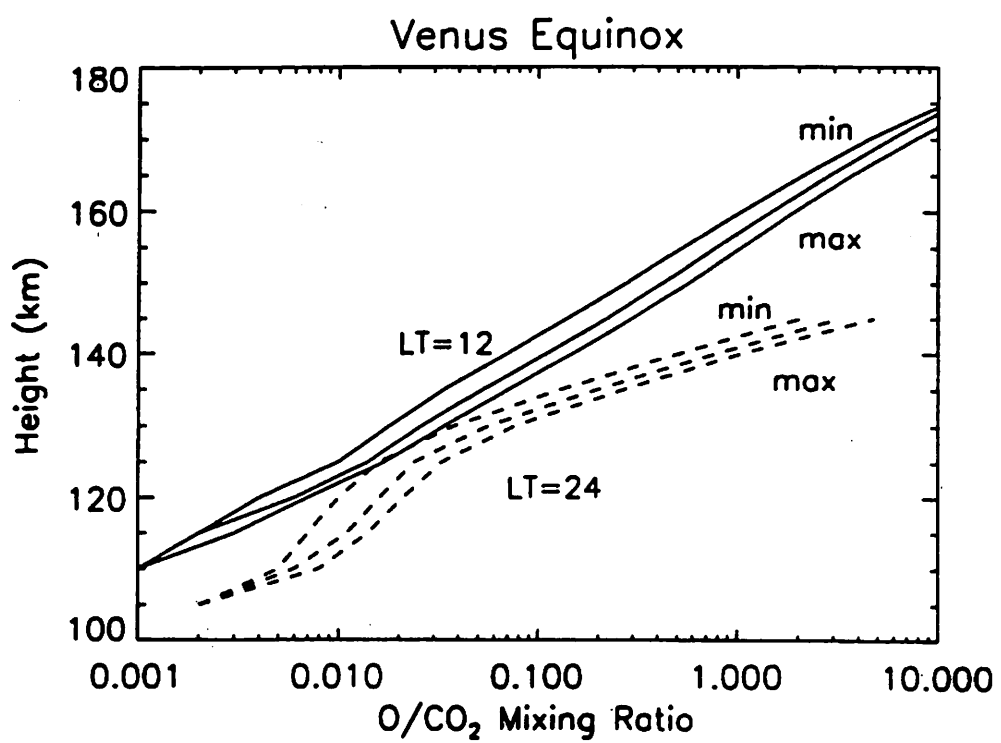
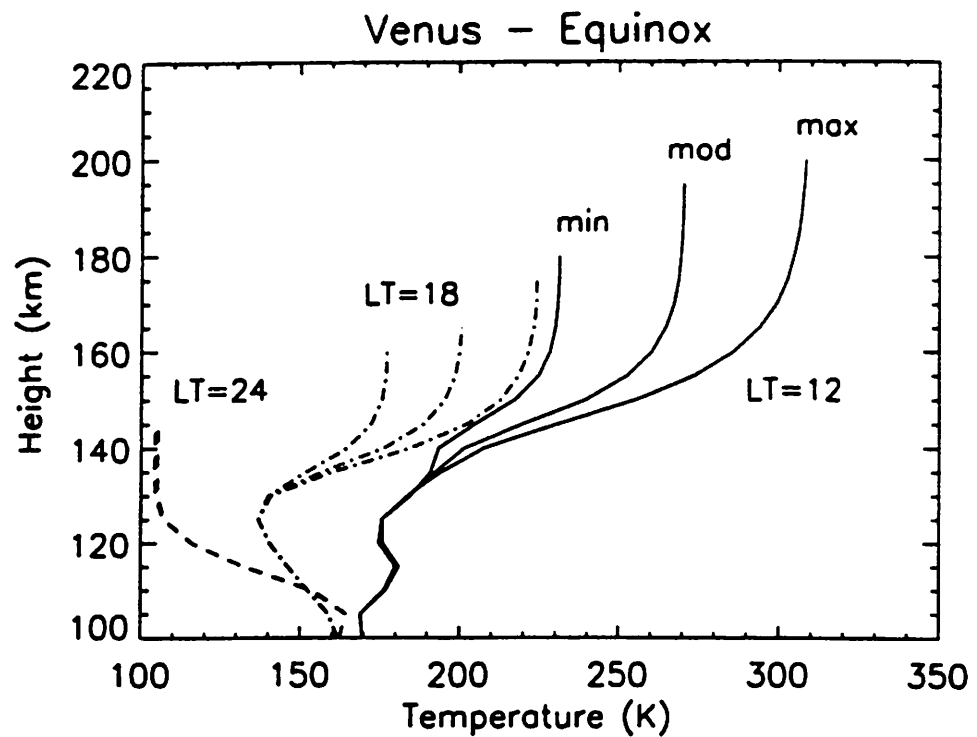
C. Specific TIEGCM Processes Included :

- Roble *et al.*, [1987] and Roble [1995] aeronomic scheme
- Self-consistent EUV/UV neutral heating calculated (non-local)
- Empirical models of high-latitude ion convection
- Empirical models of auroral particle precipitation
- Richmond *et al.*, [1992] dynamo model (electrodynamics)
- Coupling of semi-diurnal and diurnal tidal components
- Eccentricity variation as a function of season (recent)

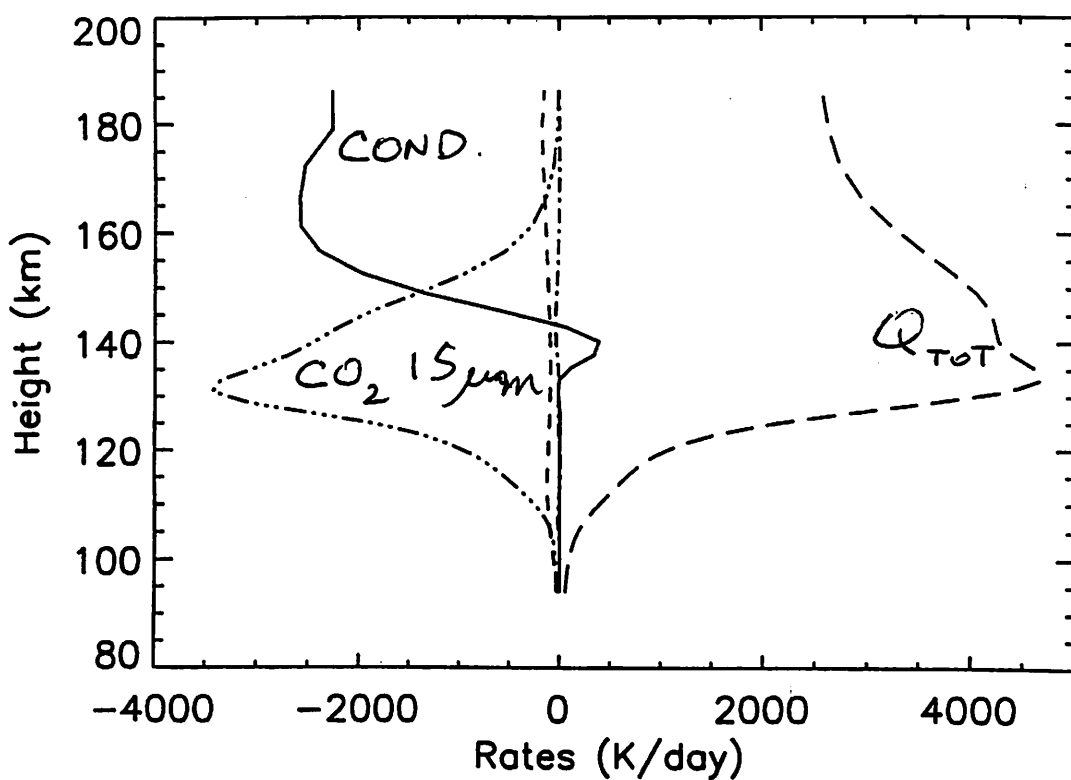
COMMON TGCM INPUTS FOR SEASONAL - SOLAR CYCLE CASES

- F10.7-cm indices used to specify standard EUV-UV fluxes
 - F10.7 = 70, 130, 200 for SMIN, SMED, SMAX cases
 - Hinteregger contrast ratio method (Solomon subroutine)
 - Fluxes from 2.0 to 200.0 nm
 - Eccentricity variations ($\pm 3\%$ Earth; $\pm 20\%$ Mars)
- Heating efficiencies specified based upon off-line calculations
 - VTGCM : EUV (20%), UV(22%)
 - MTGCM : EUV (22%), UV(22%)
 - TIEGCM : EUV (30-40% over 200-300 km; up to 60% below 200 km)
 - TIEGCM : UV(30-40%)
- Common O-CO₂ relaxation rate
 - $3.0 \times 10^{-12} \text{ cm}^3/\text{sec}$ at 300K
 - Weak temperature dependence (square root of T)
- Eddy diffusion/conduction from standard formulations. Kmax :
 - VTGCM : $1.0 \times 10^7 \text{ cm}^2/\text{sec}$ at 135 km
 - MTGCM : $1.0-1.5 \times 10^7 \text{ cm}^2/\text{sec}$ at 125 km
 - TIEGCM : $1.6 \times 10^6 \text{ cm}^2/\text{sec}$ near 100 km
- Low auroral activity parameters for Earth TIEGCM
 - Cross tail potential of 45KV
 - Integrated global power input of 16.0 GW
- Tidal parameters specified at the lower boundaries
 - MTGCM : semi-diurnal amplitudes and phases from NASA AMES MGCM
 - TIEGCM : diurnal & semi-diurnal amplitudes and phases from Forbes seasonal climatology

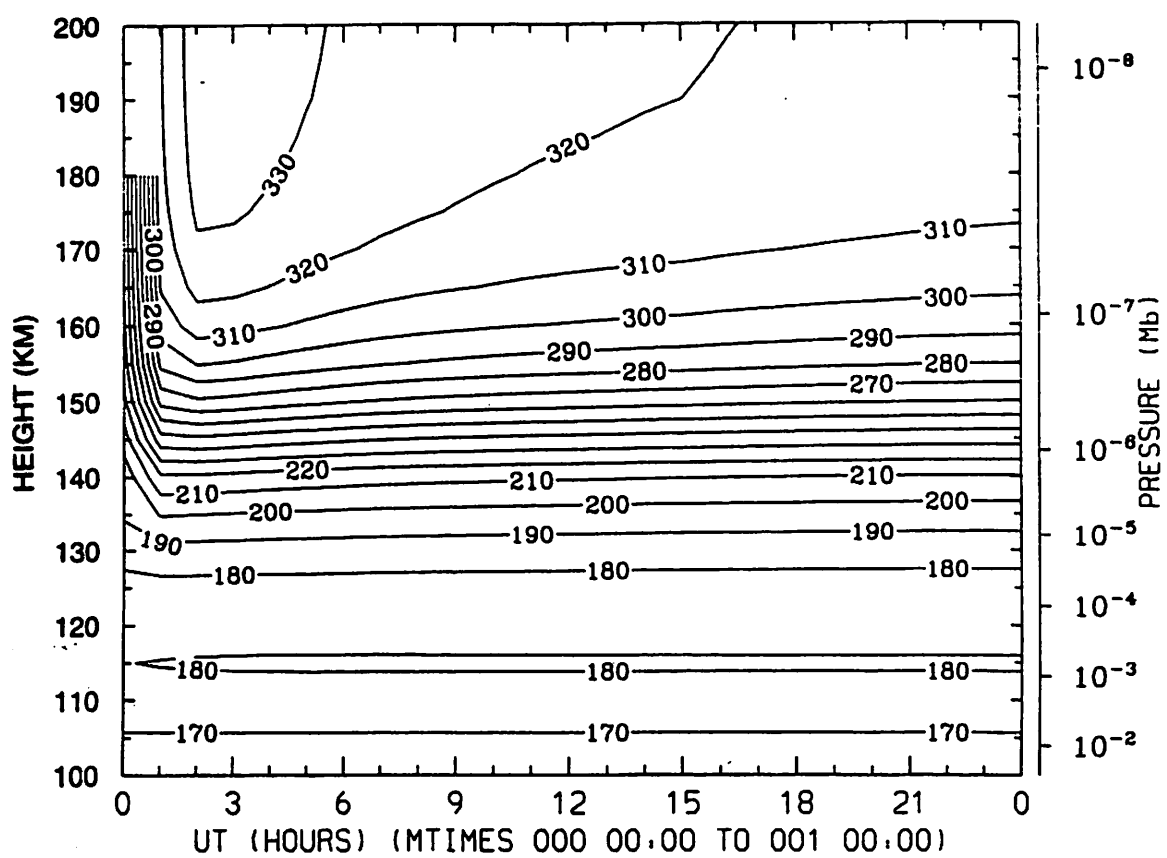
Bougher et al. (1999)



Bougher et al. (1999)
TO



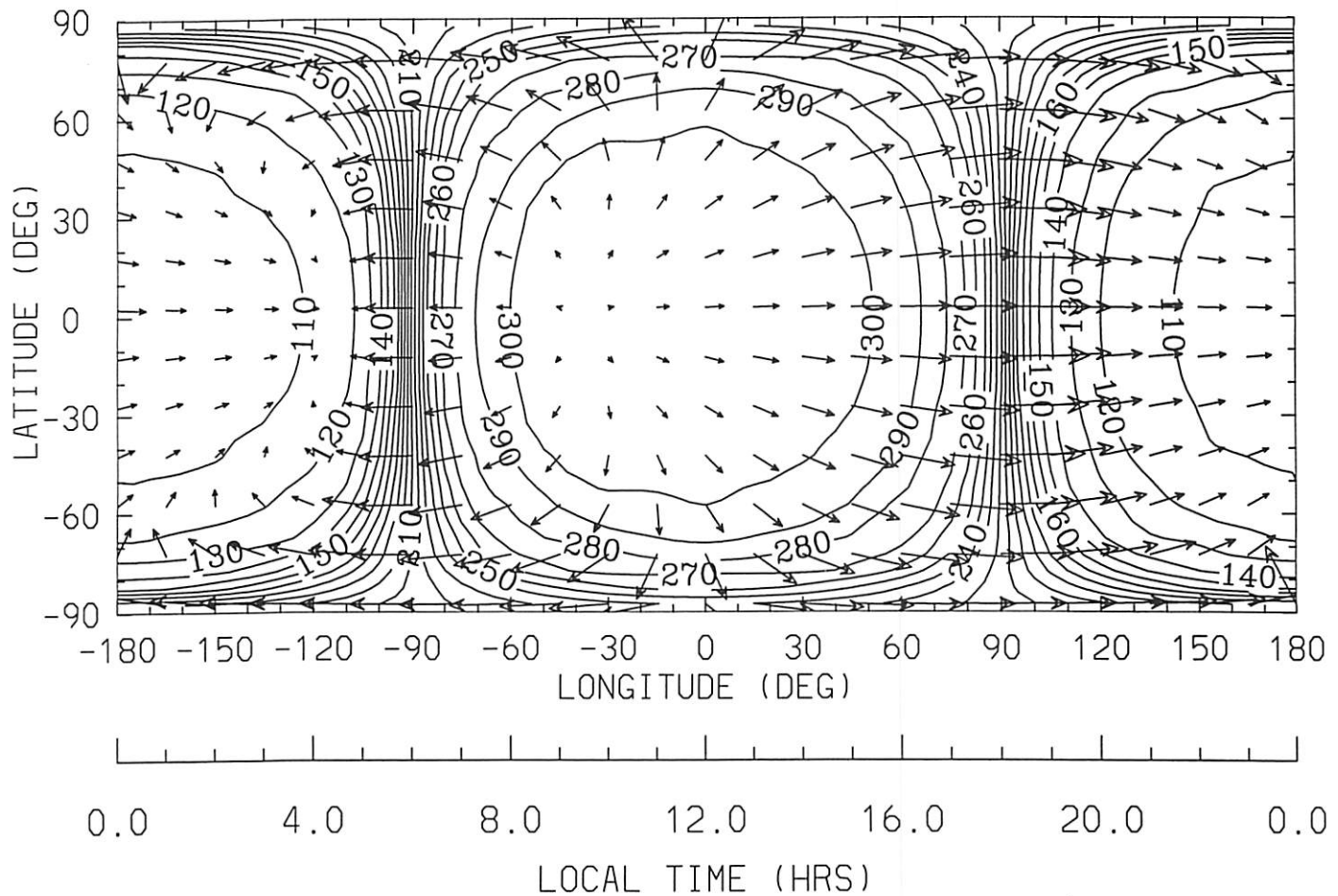
$$SLT = 12$$



VTGCM

NEUTRAL TEMPERATURE (DEG K)

UT=12.00 ZP= 7.00 AVE HT= 176.9



MIN,MAX= 1.0427E+02 3.0843E+02 INTERVAL= 1.0000E+01

VTGCM /BOUGHER/SWBV97/EQUMAX (DAY, HR, MIN= 10, 0, 0)

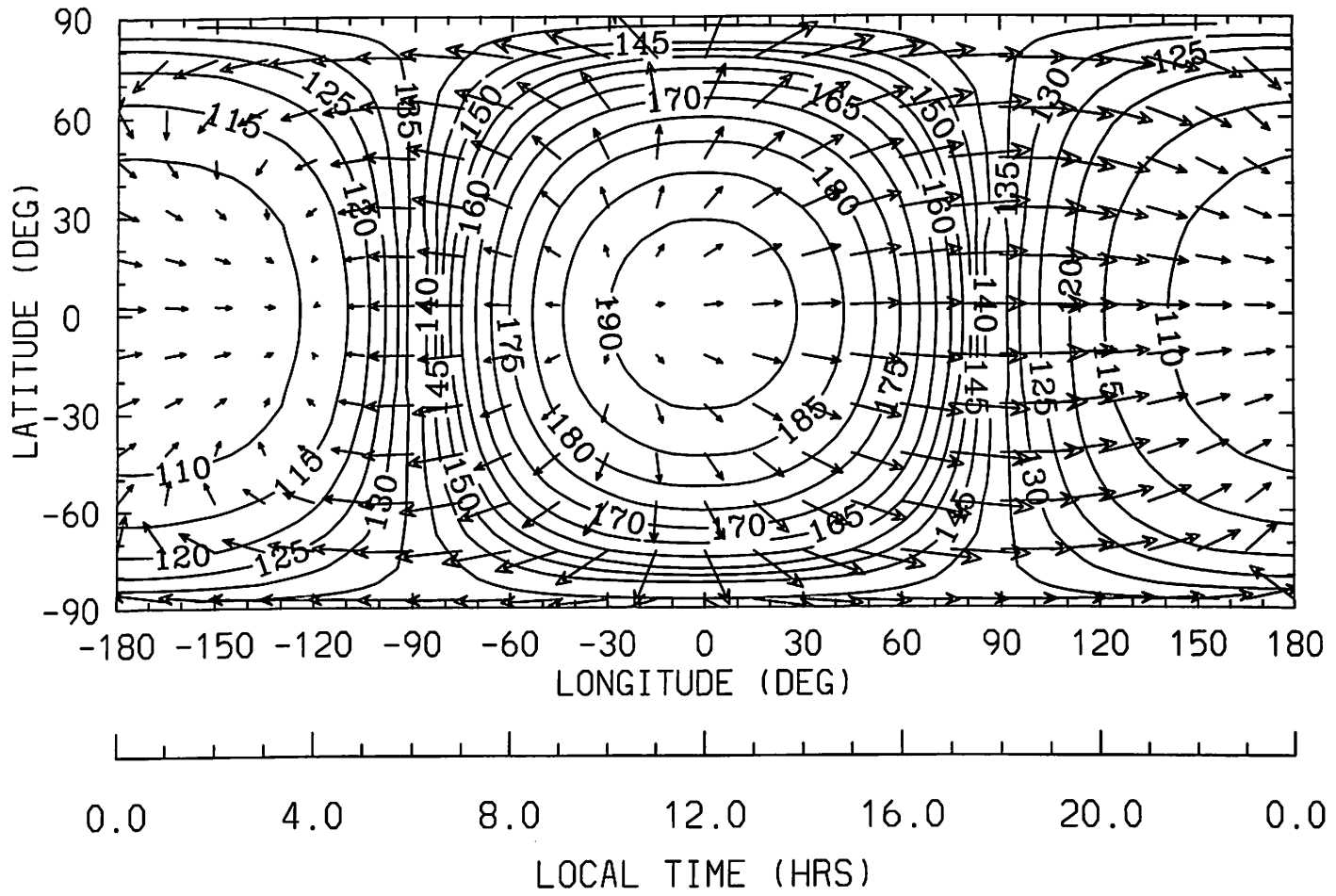
0.263E+03

$\xrightarrow{\text{UN} + \text{VN}}$

VTGCM

NEUTRAL TEMPERATURE (DEG K)

UT=12.00 ZP= 0.00 AVE HT= 129.5

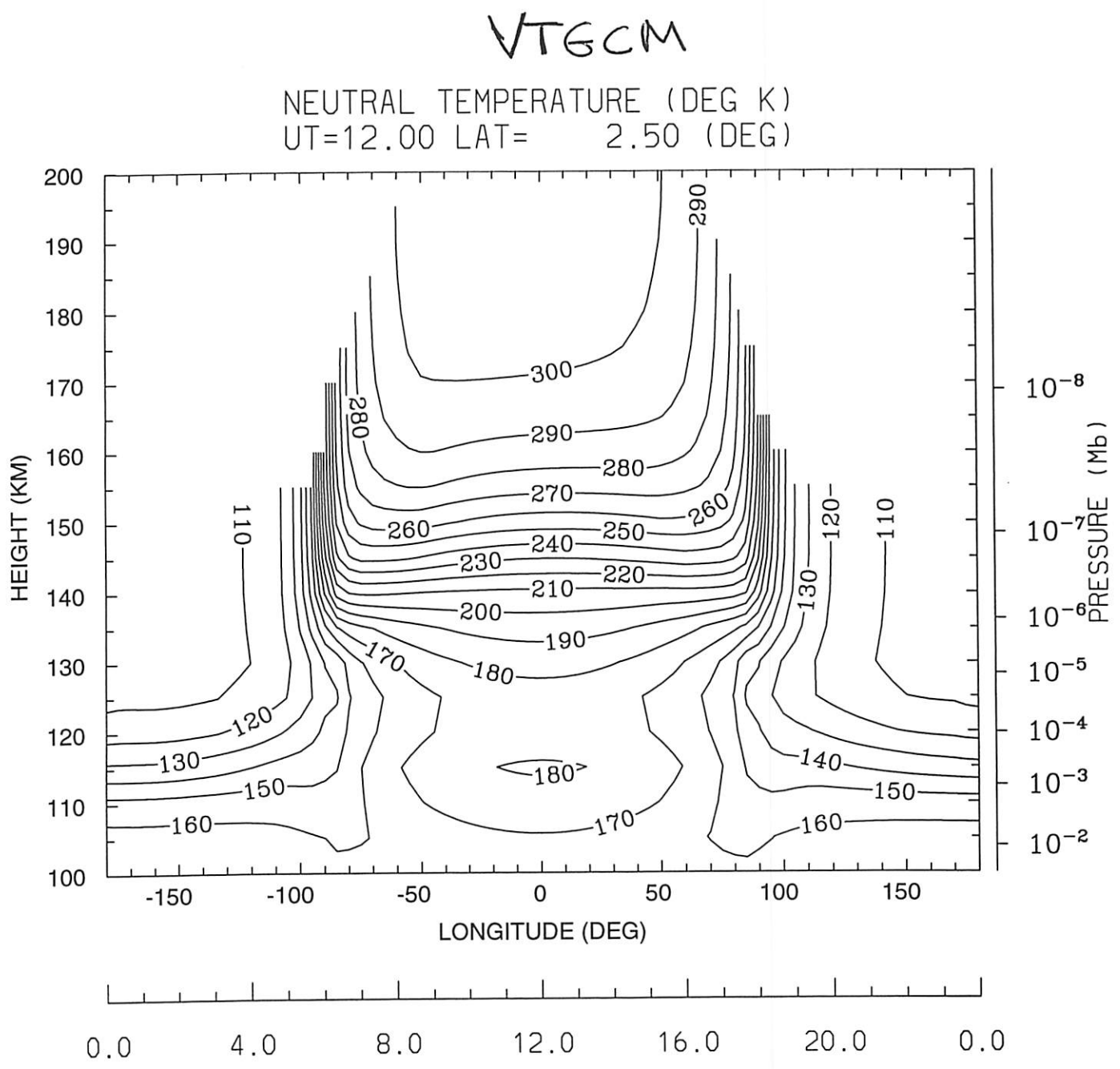


MIN,MAX= 1.0579E+02 1.9356E+02 INTERVAL= 5.0000E+00

VTGCM /BOUGHER/SWBV97/EQUMAX (DAY,HR,MIN= 10, 0, 0)

0.163E+03

$\xrightarrow{\text{UN} + \text{VN}}$



MIN,MAX= 1.0425E+02 3.0829E+02 INTERVAL= 1.0000E+01
 VTGCM /BOUGHER/SWBV97/EQUMAX (DAY,HR,MIN= 10, 0, 0)

Bougher and Borucki (94)

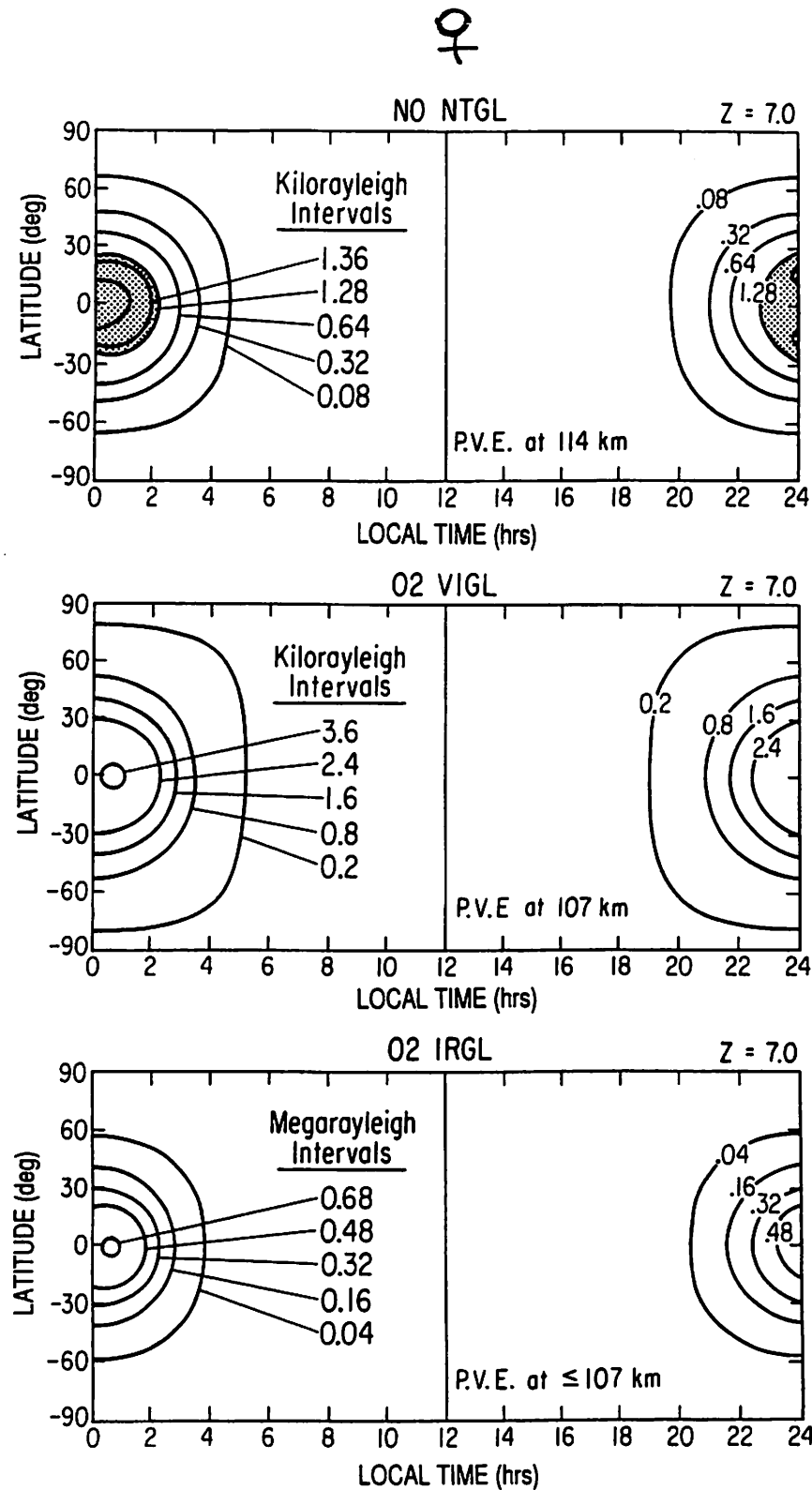
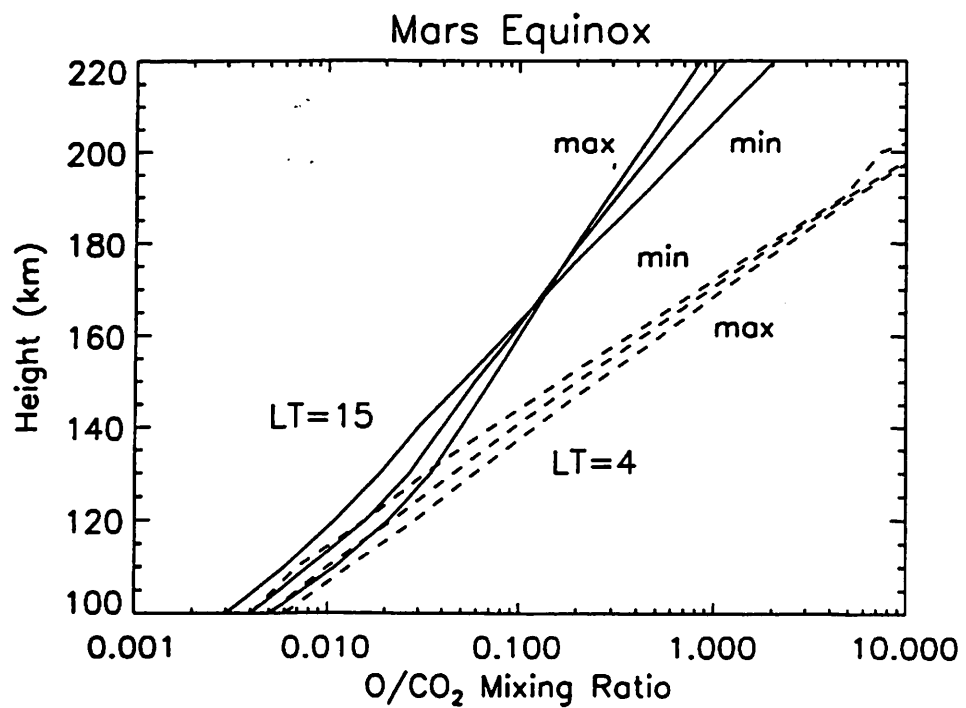
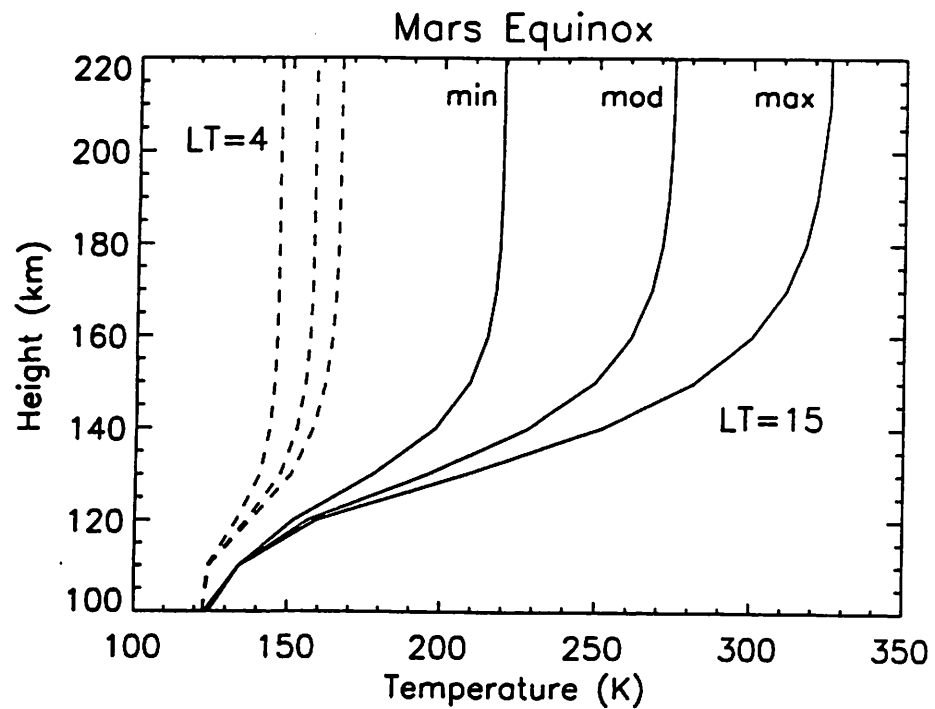
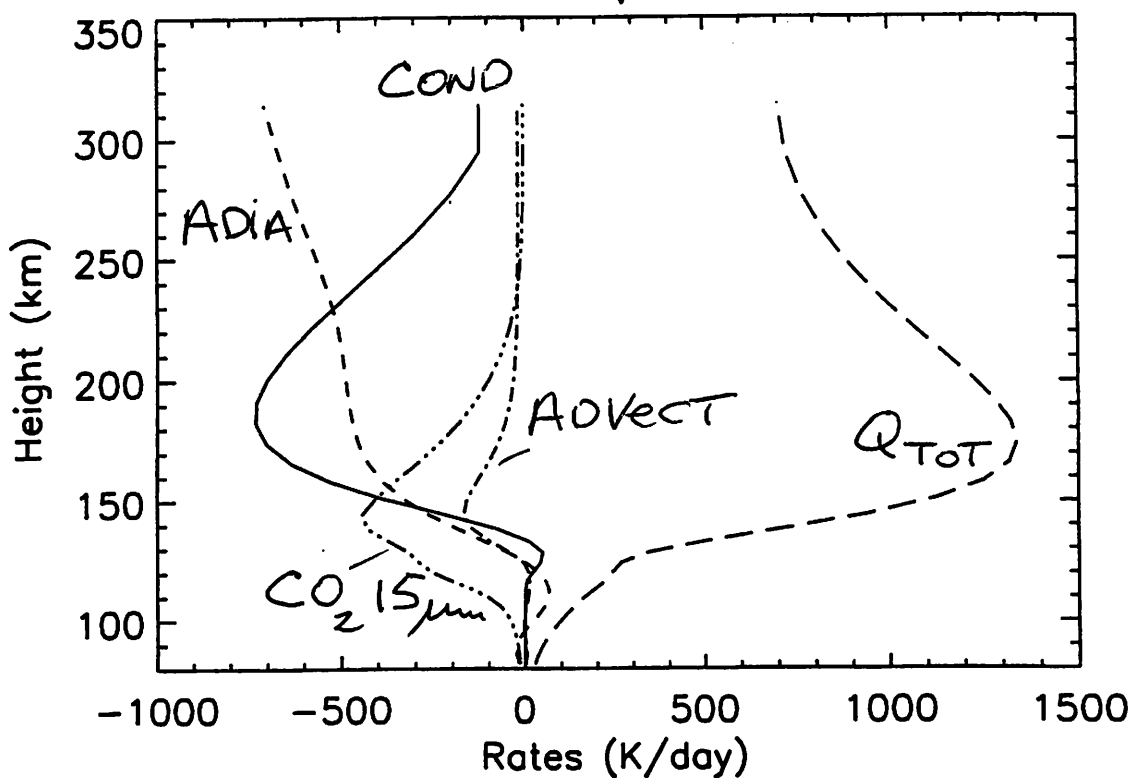


Figure 6. The VTGCM SMAX model. A set of night airglow distributions corresponding to the wind field is given for: (top) the NO(0,1) δ -band emission at 198 nm (NO NTGL); (middle) the O₂ Herzberg II visible nightglow over 400 to 800 nm (O₂ VIGL); and (bottom) the O₂ 1.27- μ m infrared nightglow (O₂ IRGL). The peak volume emission (PVE) rate altitude is indicated for each nightglow distribution.

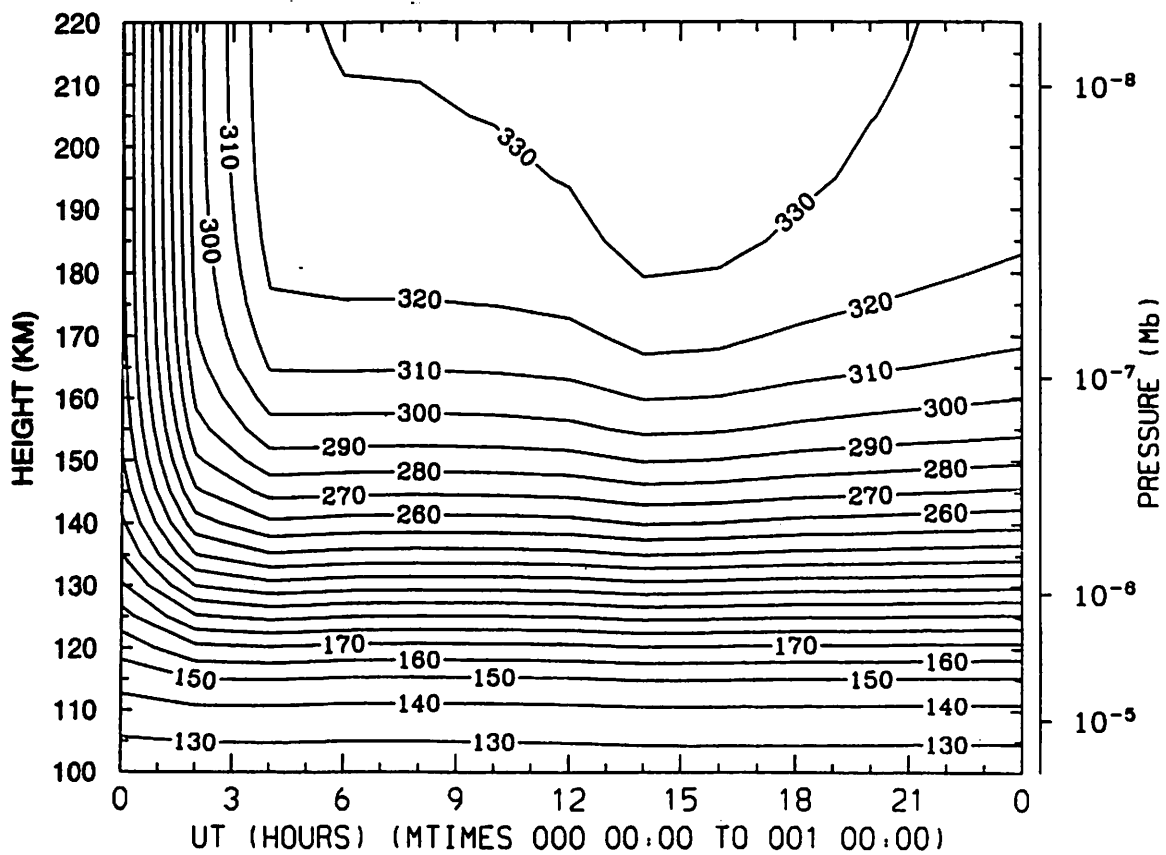
Bougher et al. (1999)



Bougher et al. (1999)



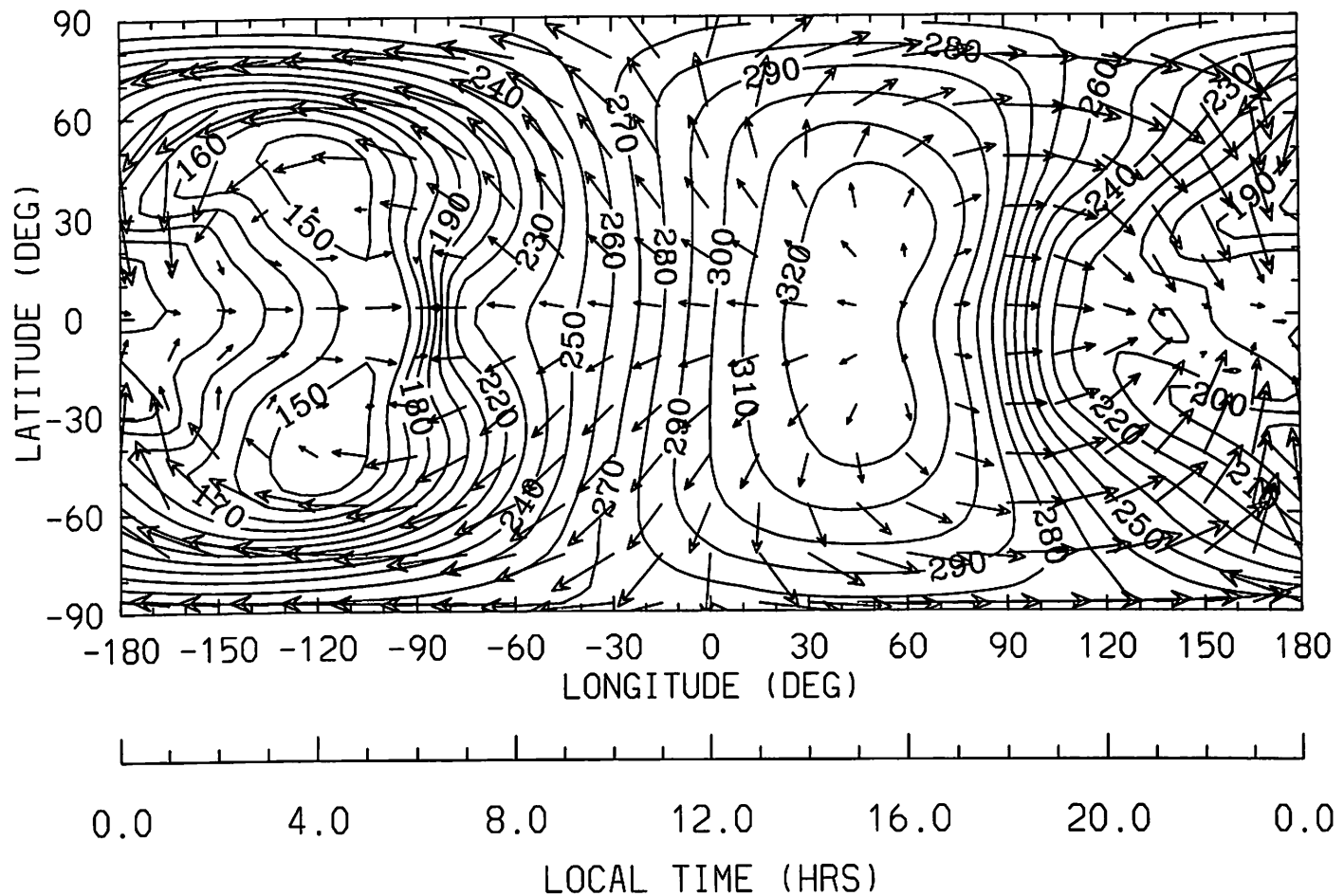
SLT = 15



MTGCM

NEUTRAL TEMPERATURE (DEG K)

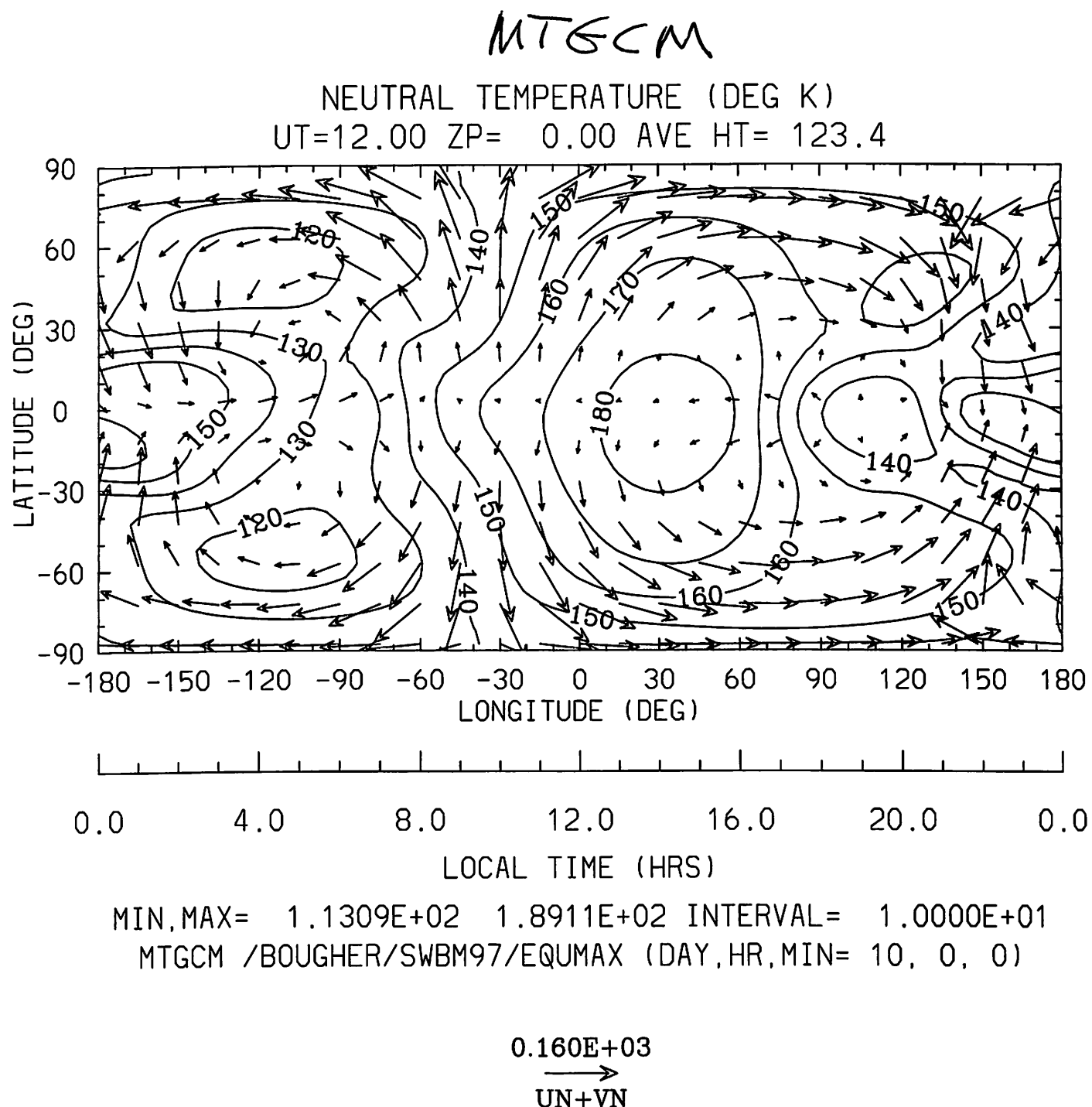
UT=12.00 ZP= 6.00 AVE HT= 216.0

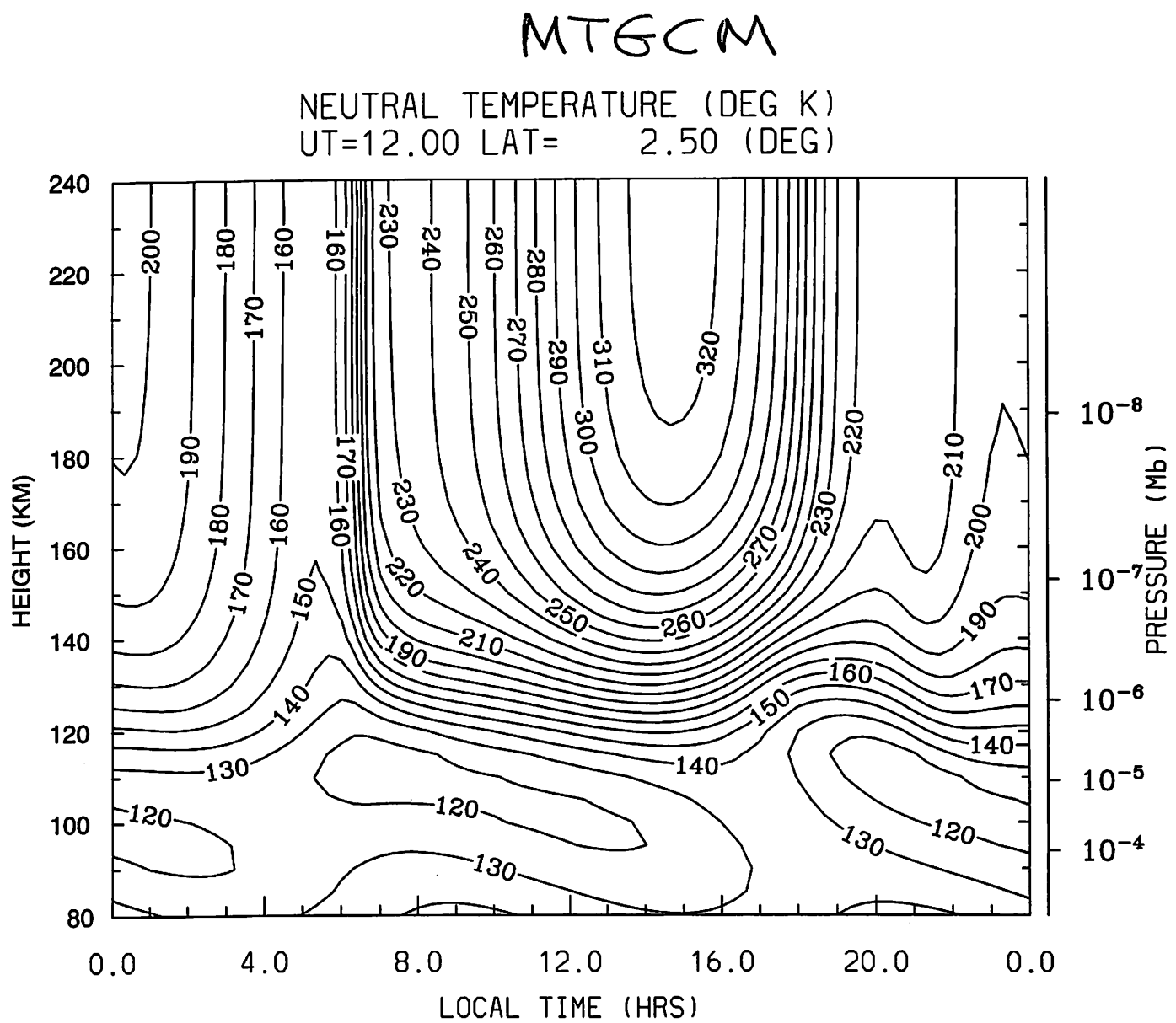


MIN,MAX= 1.4060E+02 3.2752E+02 INTERVAL= 1.0000E+01

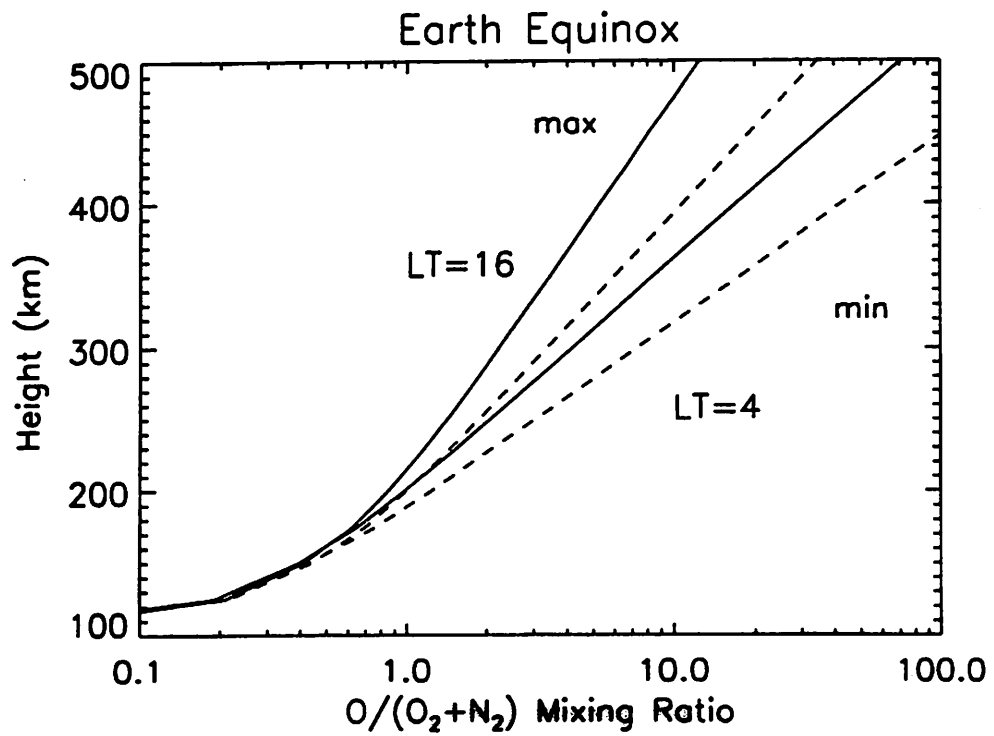
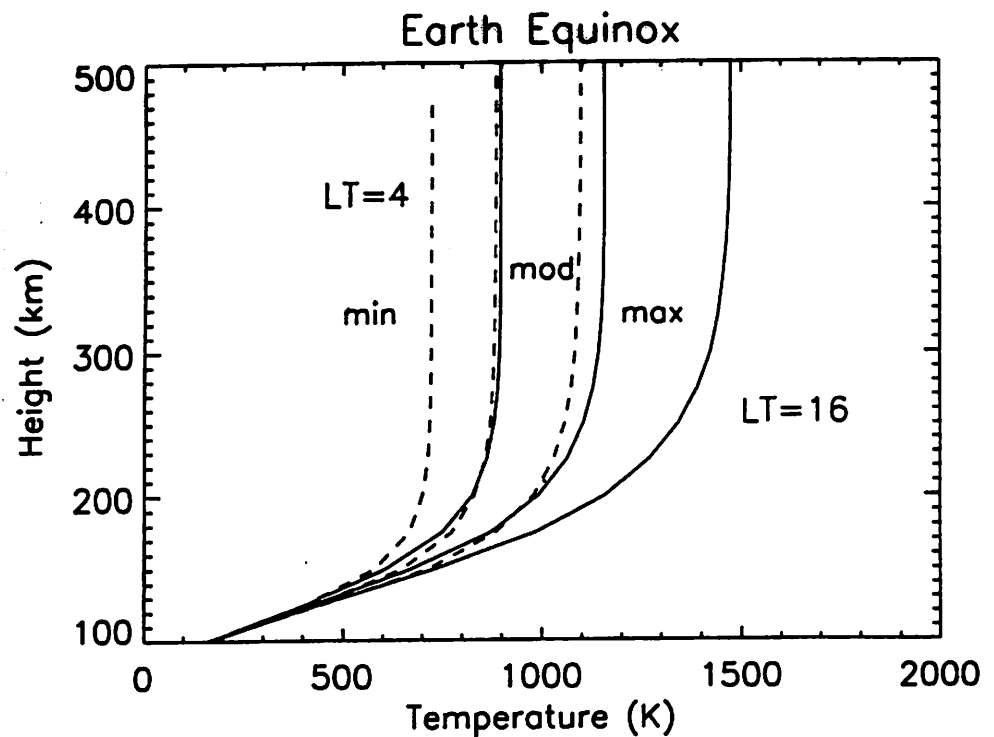
MTGCM /BOUGHER/SWBM97/EQUMAX (DAY,HR,MIN= 10, 0, 0)

0.305E+03
→
UN+VN

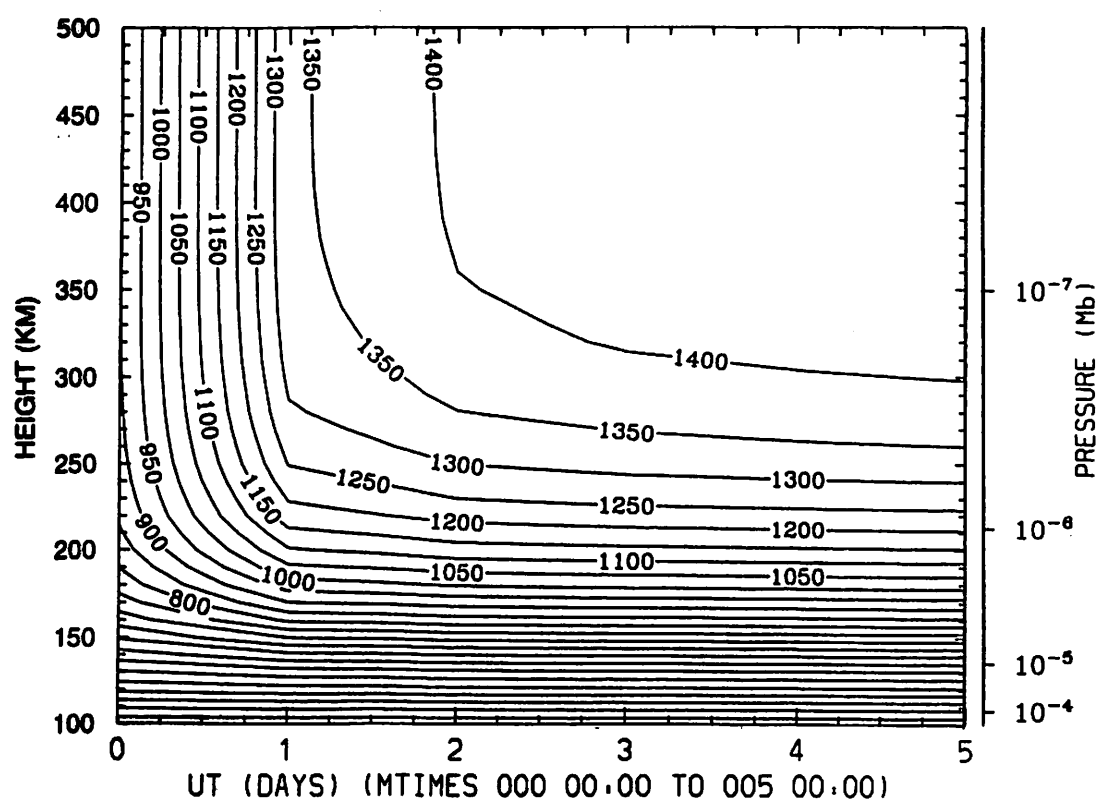
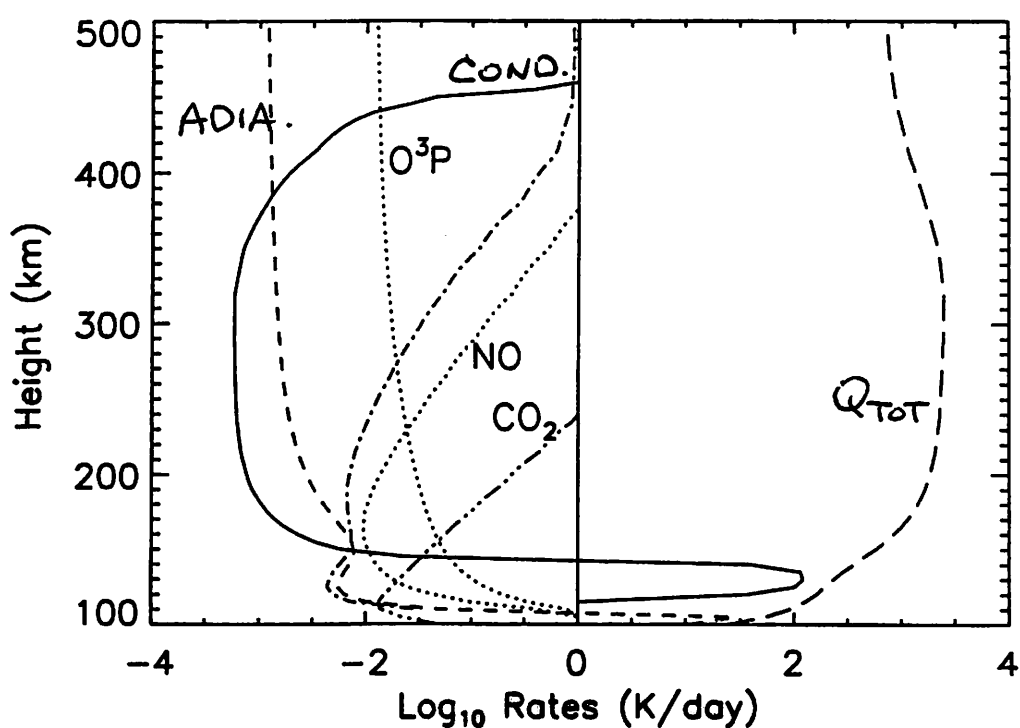




MIN,MAX= 1.1360E+02 3.2596E+02 INTERVAL= 1.0000E+01
 MTGCM /BOUGHER/SWBM97/EQUMAX (DAY,HR,MIN= 10, 0, 0)



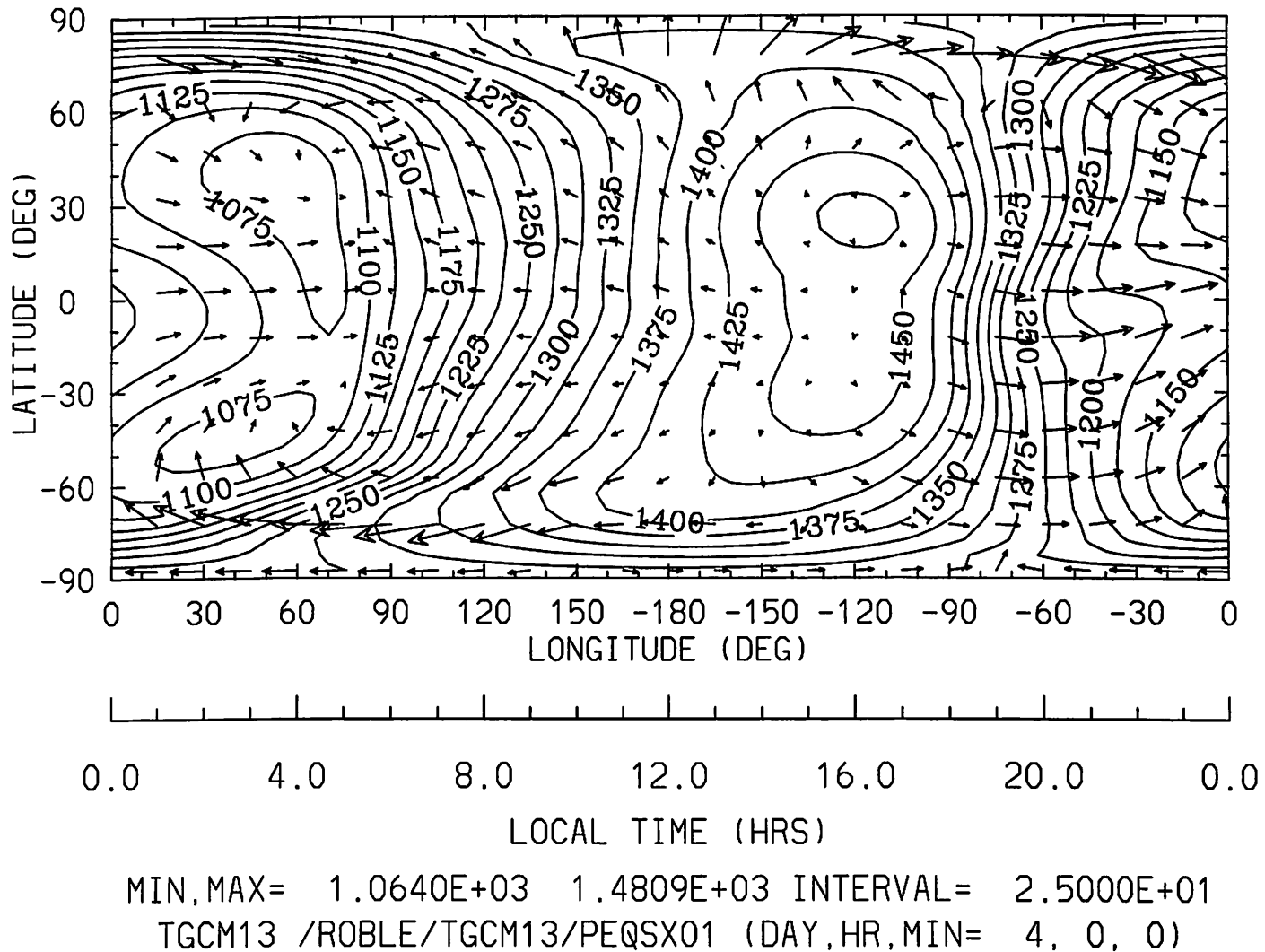
Bouger et al., (99b)



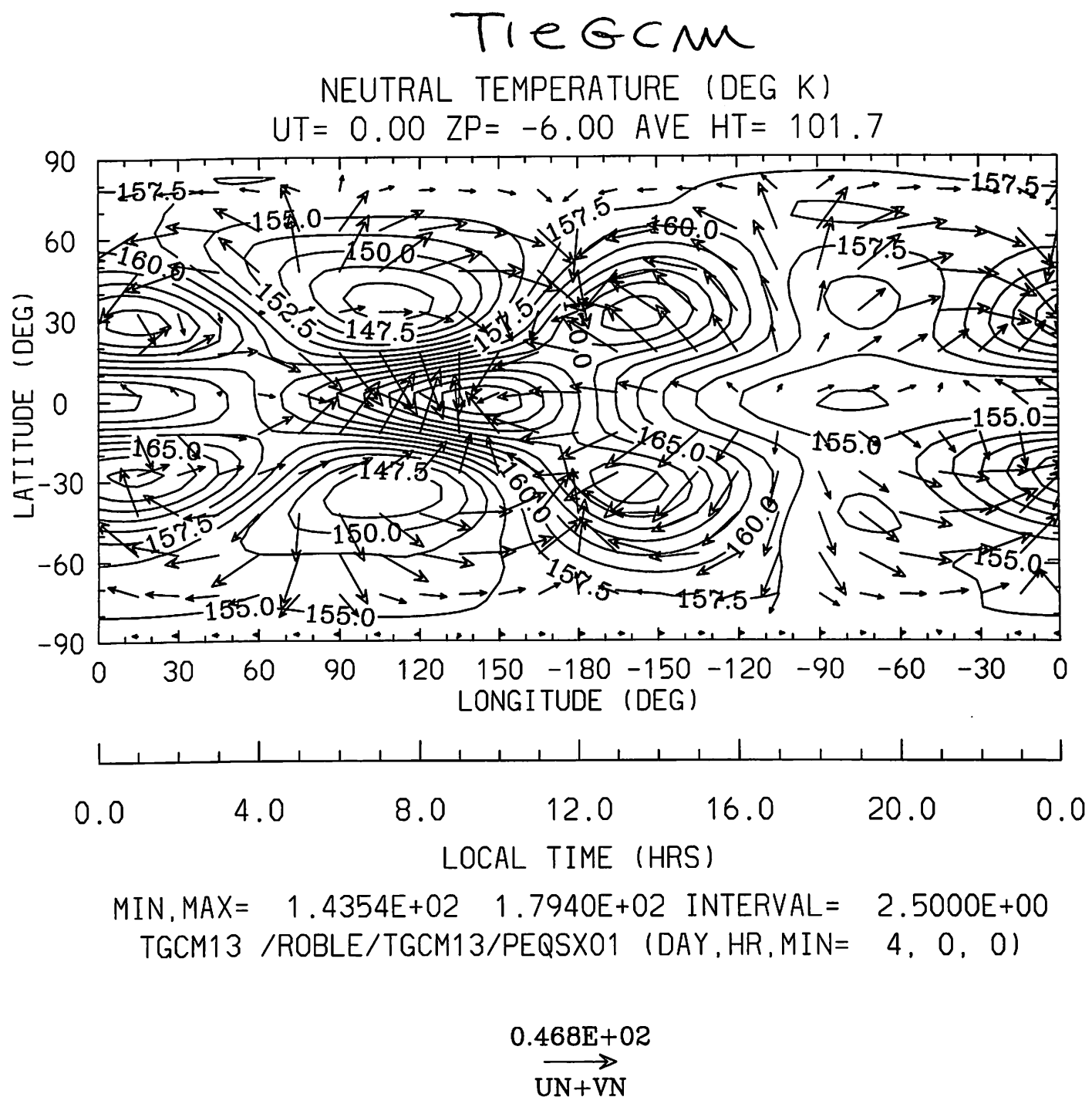
TieGCM

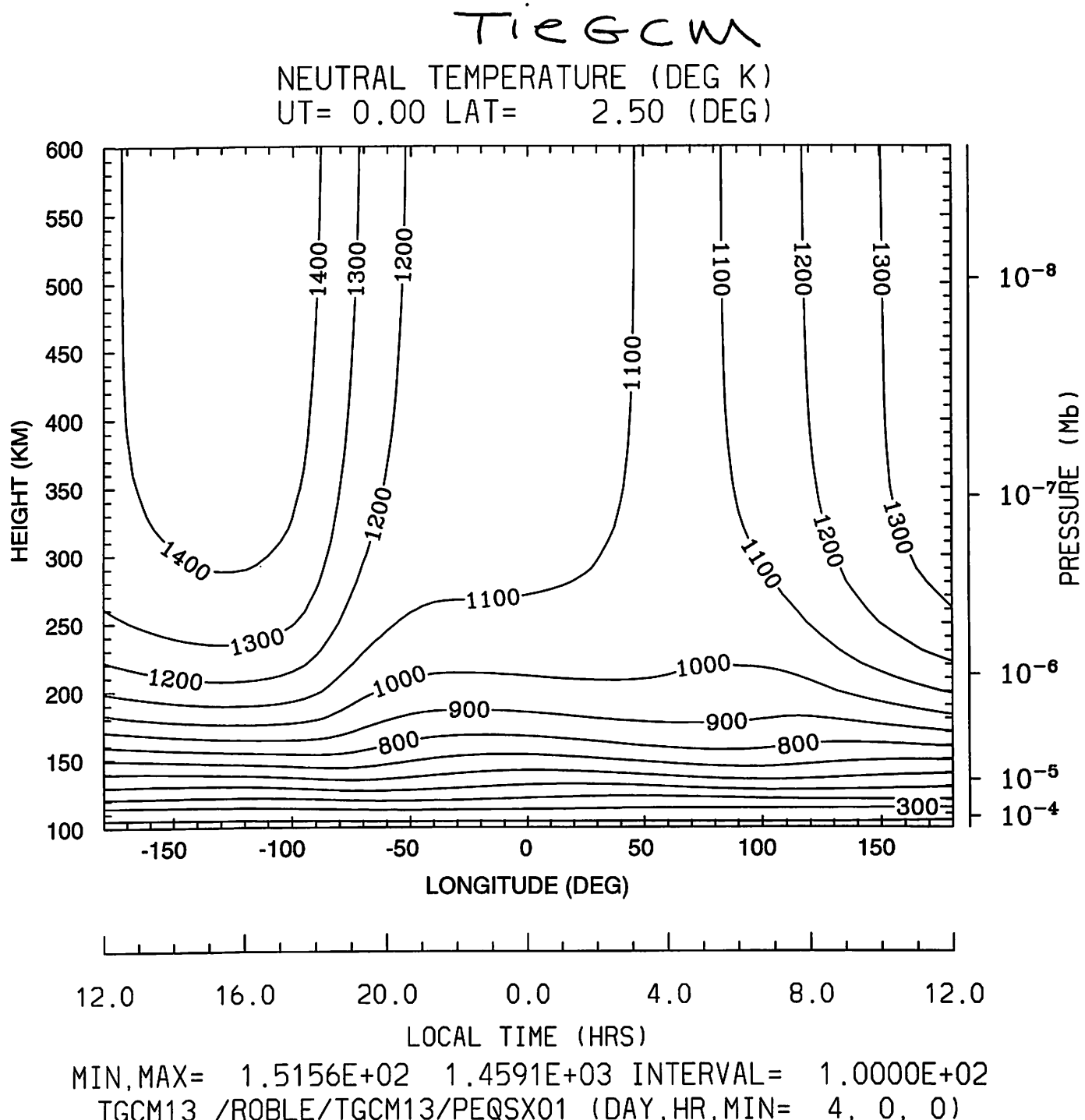
NEUTRAL TEMPERATURE (DEG K)

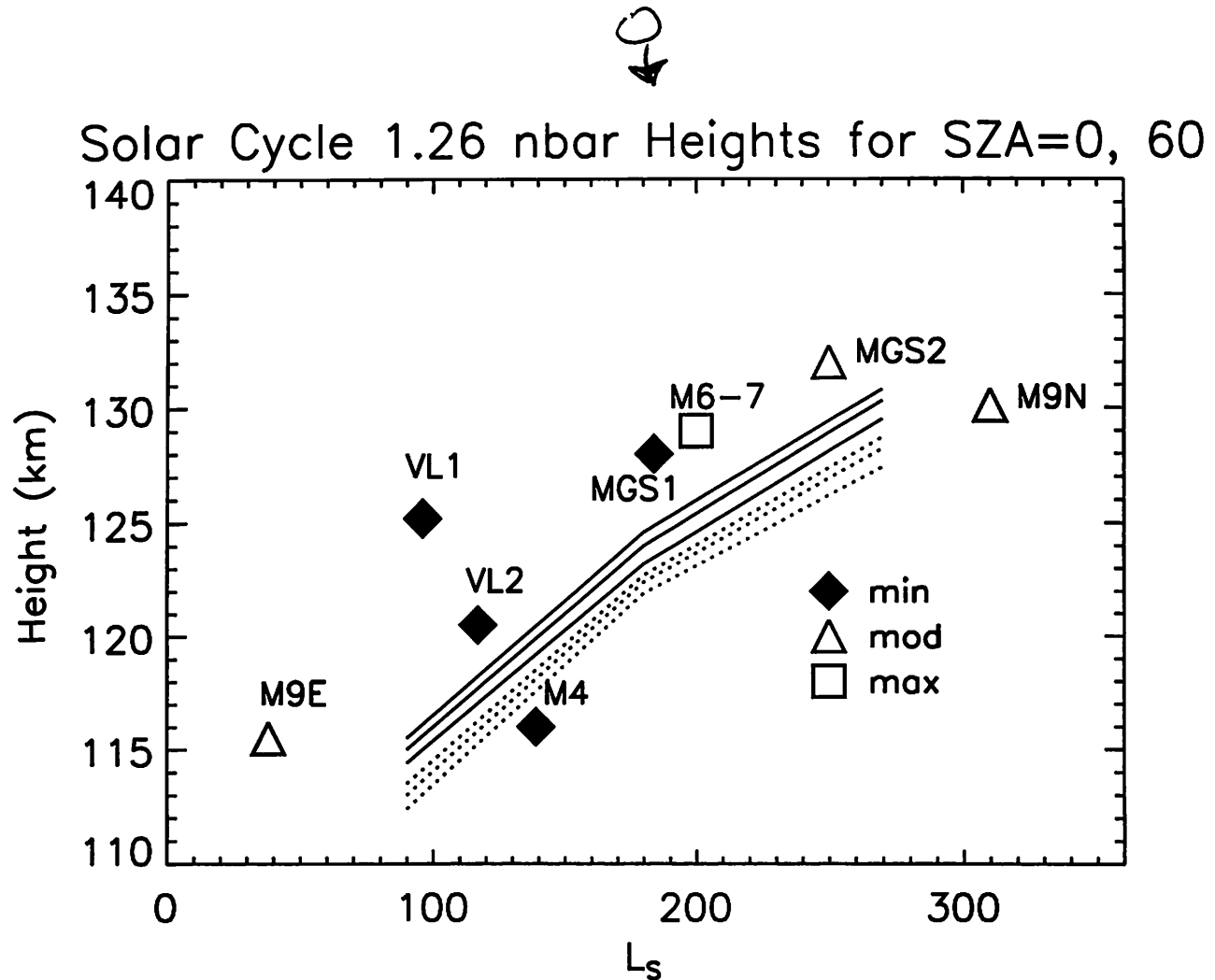
UT= 0.00 ZP= 7.00 AVE HT= 732.5



$$0.477E+03 \xrightarrow{\hspace{1cm}} \text{UN} + \text{VN}$$





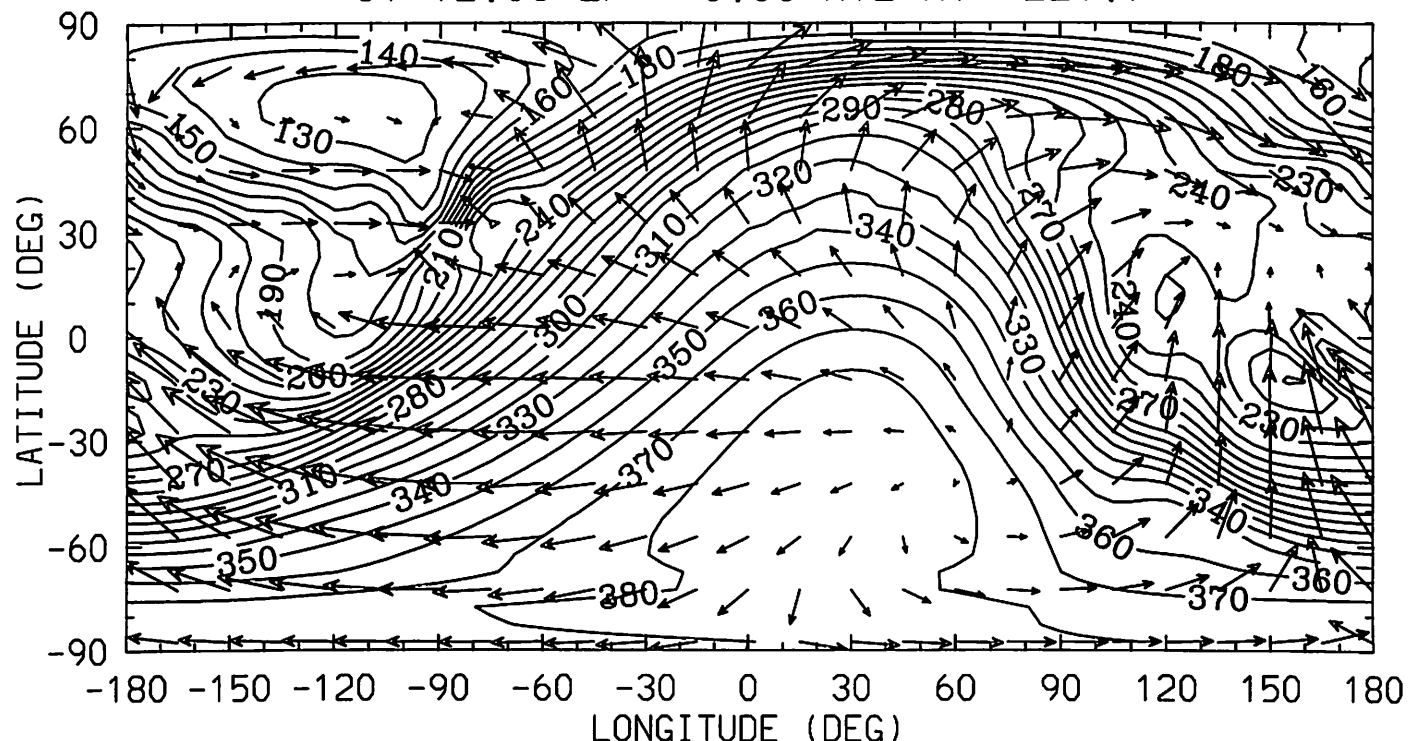


Bougger *et al.*, (00)

MTGCM

$L_s = 270^\circ / \text{MAX}$

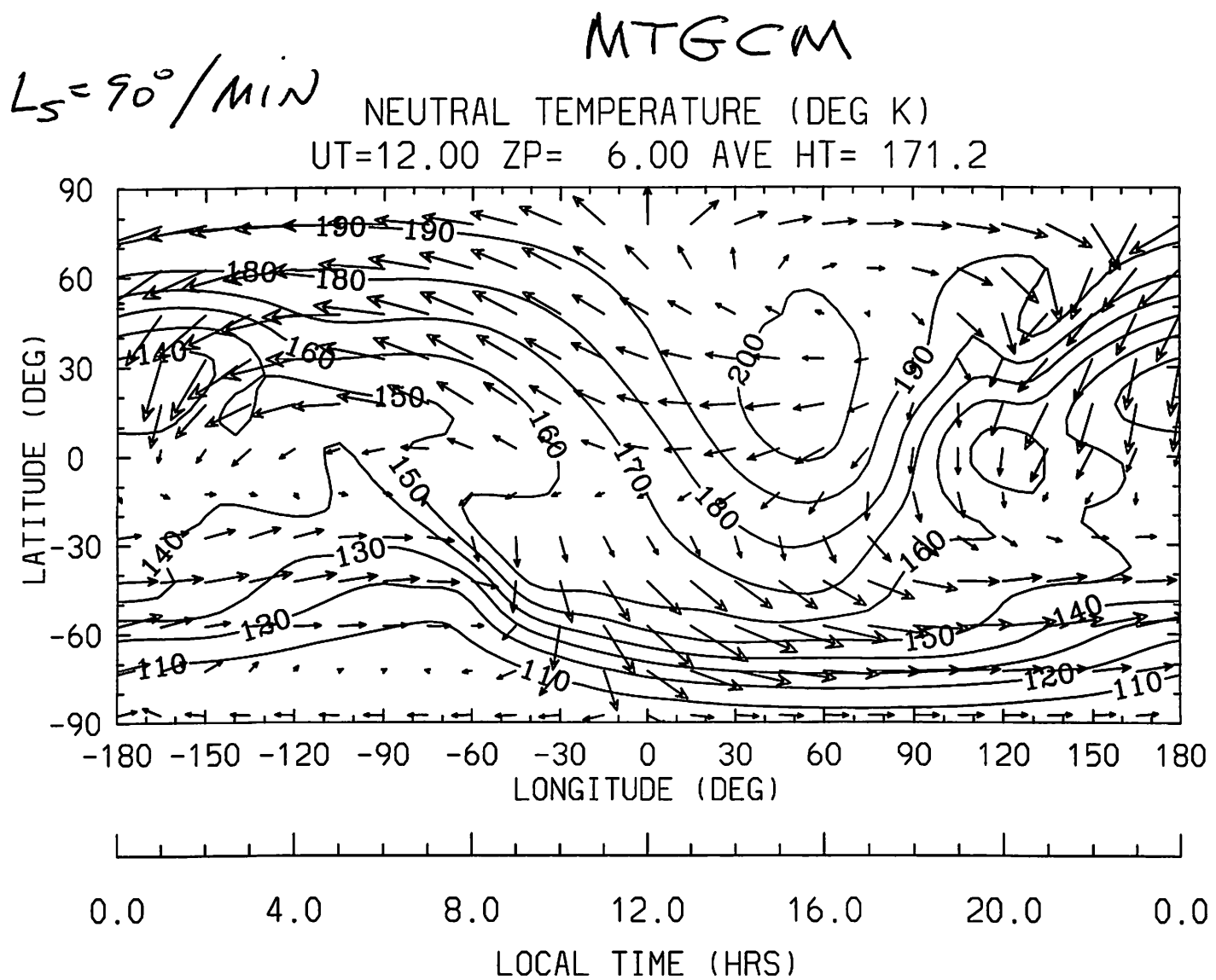
NEUTRAL TEMPERATURE (DEG K)
UT=12.00 ZP= 6.00 AVE HT= 229.7



0.0 4.0 8.0 12.0 16.0 20.0 0.0
LOCAL TIME (HRS)

MIN,MAX= 1.2360E+02 3.8879E+02 INTERVAL= 1.0000E+01
MTGCM /BOUGHER/SWBM97/SSLMAX (DAY,HR,MIN= 5, 0, 0)

0.403E+03
→
UN+VN



MIN,MAX= 1.0143E+02 2.0452E+02 INTERVAL= 1.0000E+01

MTGCM /BOUGHER/SWBM97/NSLMIN (DAY,HR,MIN= 5, 0, 0)

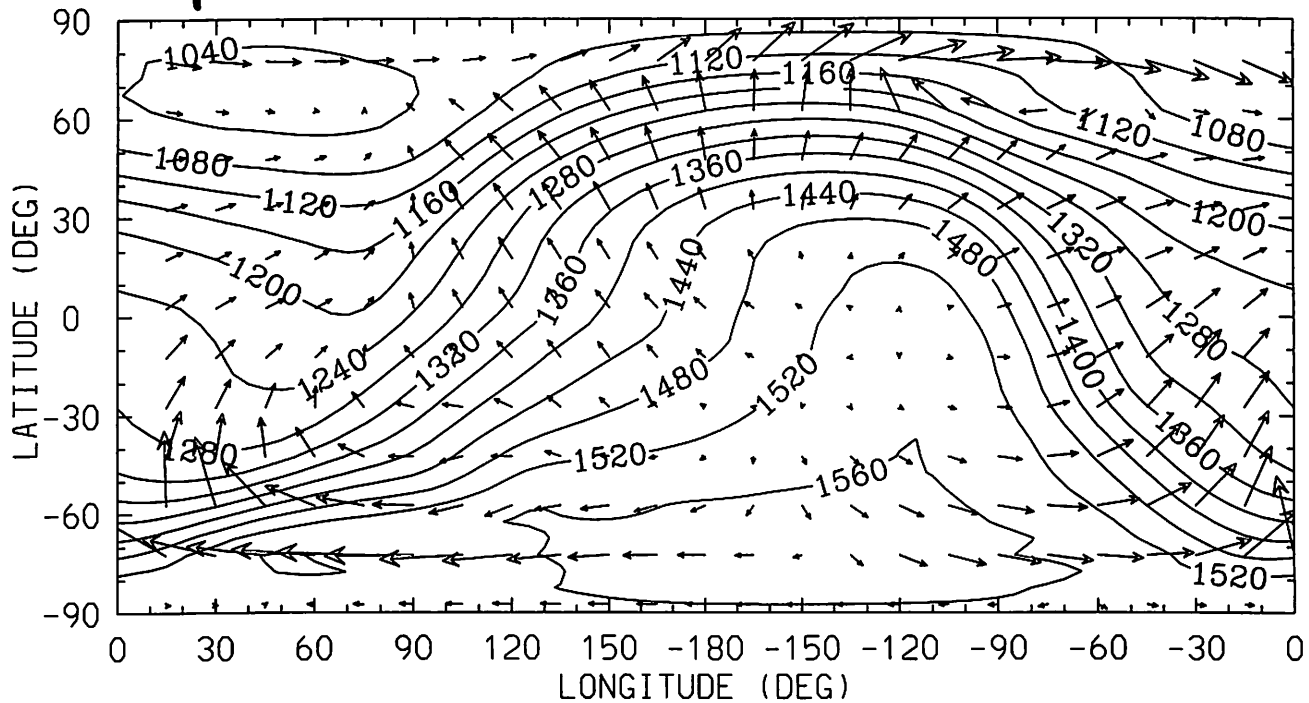
$0.216\text{E}+03$
 $\xrightarrow{\hspace{1cm}}$
 UN+VN

Bougher et al., (00)

TIEGCM

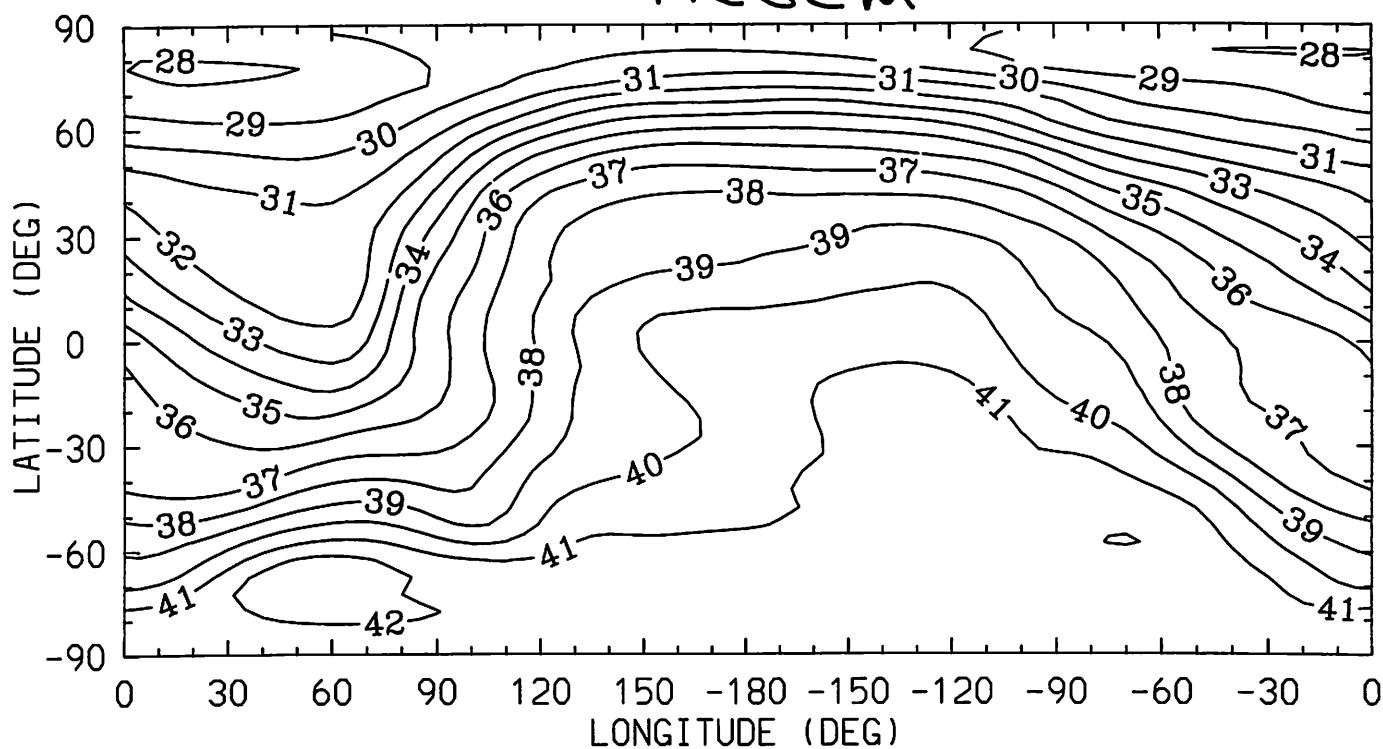
DEC/MAX

NEUTRAL TEMPERATURE (DEG K)
UT= 0.00 ZP= 7.00 AVE HT= 756.5

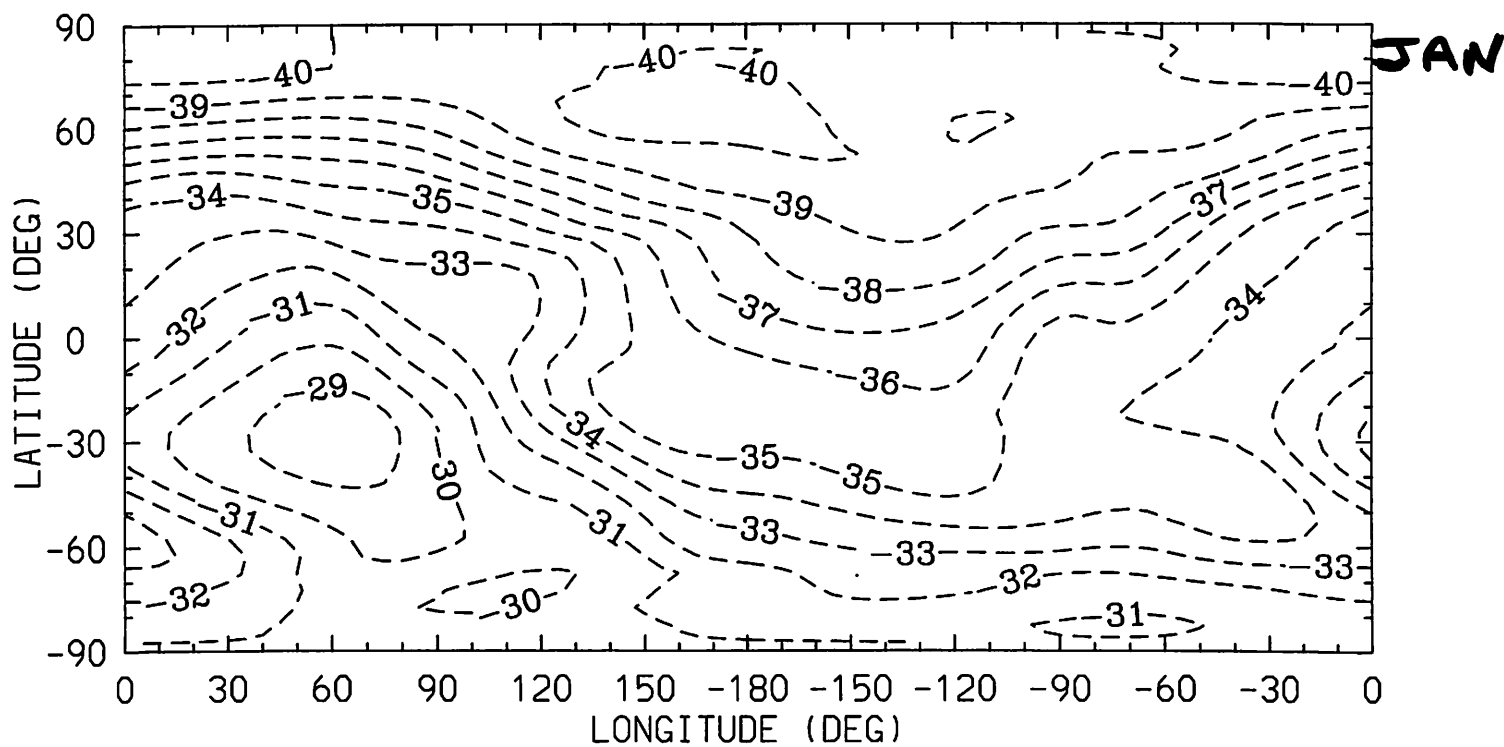


RAW DIFFS: NEUTRAL TEMPERATURE (DEG K)

TIEGC M



DEC



JAN

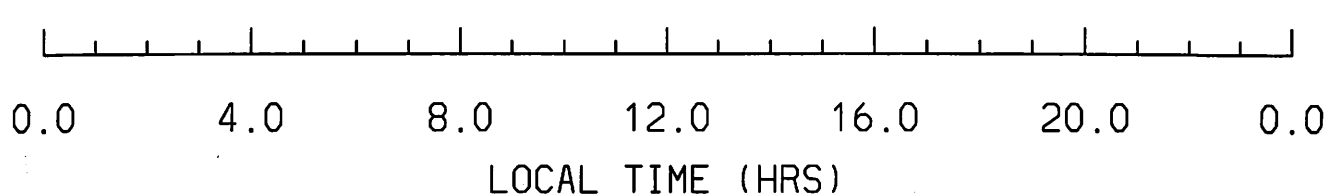


Table 1a. Terrestrial Planet Parameters

Parameter	Earth	Venus	Mars
Gravity, cm/s ²	982	888	373
Heliocentric distance AU	1.0	0.72	1.38-1.67
Radius, km	6371	6050	3396
Ω , rad/s	7.3(-5)	3.0(-7)	7.1(-5)
Magnetic dipole moment (wrt Earth)	1.0	$\leq 4.0(-5)$	$\leq 2.5(-5)$
Obliquity, deg	23.5	1-3	25.0

Table 1b. Implications of Parameters

Effect	Earth	Venus	Mars
Scale heights, km	10-50	4-12	8-22
Major EUV heating, km	~ 200 -300 broad	~ 140 -160 narrow	120-160 intermediate
O Abundance (ion peak)	$\sim 40\%$	~ 7 -20%	~ 1 -4%
CO ₂ 15- μ m cooling	≤ 130 km	≤ 160 km	≤ 125 -130 km
Dayside thermostat	conduction	CO ₂ cooling	winds/conduction
Dayside solar cycle T	900-1500 K	230-310 K	220-325 K
Rotational forces	important	negligible	important
Cryosphere	no	yes	no
Auroral/Joule heating	yes	no	no
Seasons	yes	no	yes

Key Comparative Planetary Thermospheres Problems

I. The role of CO₂ cooling in the upper atmospheres of Venus, Earth, and Mars

- Confirm a fast de-activation rate (O-CO₂ collisions) for all 3-planets
- Quantify the CO₂ cooling rates in thermal budgets of these upper atmospheres
- Confirm the mechanism underlying the Earth 'falling sky' effects

II. The coupling of the lower and upper atmospheres of Earth and Mars

- Quantify the combined/individual impact of tides, other planetary-scale waves, and gravity waves upon the Mesosphere-Thermosphere-Ionosphere (MTI) regions of both these planets as a function of season, solar cycle, latitude, etc.
- Improve predictions of the Mars upper atmosphere for aerobraking exercises

III. Large scale circulation patterns in the Venus, Earth and Mars upper atmospheres

- Role of fundamental planetary parameters in driving wind patterns
- Quantify how the changing solar EUV/UV fluxes alter the thermospheric circulation patterns of these 3-planets over the solar cycle?

IV. Super-rotation in planetary atmosphere (Venus, Earth, Titan, etc).

- Ascertain what planetary conditions favor the generation of such SR winds and why the SR wind magnitudes differ on various planets

V. Atmospheric escape processes for Venus, Earth, and Mars

- Quantify of the present rates of escape for the various mechanisms proposed as spacecraft data become available
- Extrapolate these mechanisms into the past (using proposed young sun EUV/UV/IR fluxes) to estimate the amount of water lost from Venus, Earth, and Mars since the cessation of early heavy bombardment.
- Answer key questions of atmosphere and climate evolution such as:
 - (1) Was Mars' early climate warm and wet? How warm and how wet? What conditions might have supported such a climate?
 - (2) Where has all the water gone that is thought to have formed the Mars fluvial features?
 - (3) Where has all the Venus water gone that its D/H ratio suggests must have once been present on the planet?

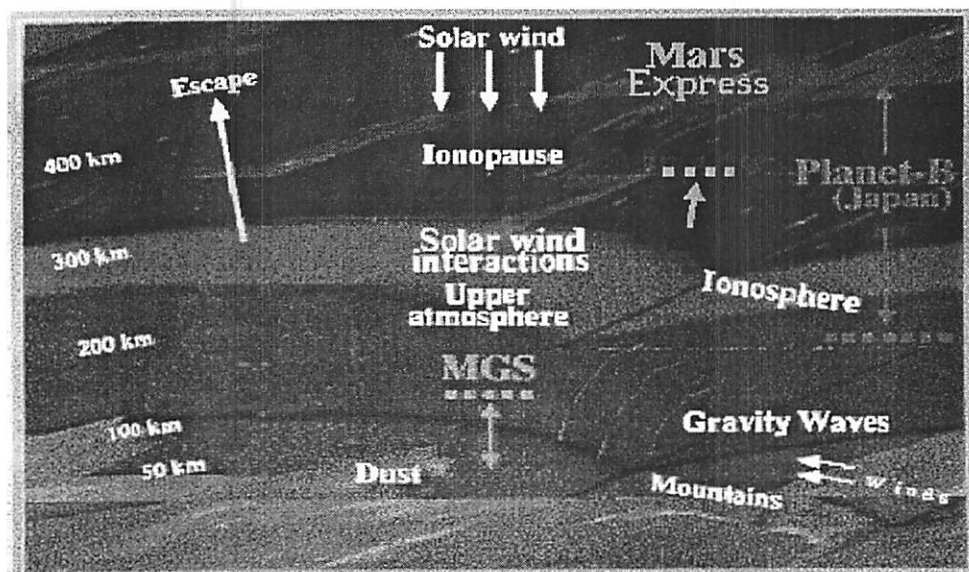
VI. Solar wind interaction with non-magnetic (Venus, Mars) versus magnetic (Earth, Jupiter, Saturn, etc.) planets

- Compare magnetospheric processes on Earth and Jupiter (magnetospheric convection driving ion drifts; particle precipitation; auroral processes giving rise to airglow features and driving neutral winds)
- Quantify the specific processes that enable the non-magnetic planets to partially or totally stand off the solar wind

Archives of Images and Tables for Venus, Earth, and Mars Thermospheres

Dr. Stephen W. Bougher

Lunar and Planetary Laboratory - University of Arizona



Martian Atmosphere

At this website, we present recent model results that illustrate the thermal, compositional and dynamical responses of the upper atmospheres of Venus, Earth, and Mars to solar EUV-UV flux variability making use of the Venus VTGCM, the Earth TIEGCM, and the Mars MTGCM three-dimensional models. Each of these models has been developed and exercised at the National Center for Atmospheric Research (NCAR) using its CRAY computers.

[... read more](#)

<http://www.lpl.arizona.edu/hsengel/thermo.html>

Archives of Thermospheric Model Runs

JOURNAL OF GEOPHYSICAL RESEARCH, VOL. 104, NO. E7, PAGES 16,591–16,611, JULY 25, 1999

Comparative terrestrial planet thermospheres 2. Solar cycle variation of global structure and winds at equinox

S. W. Bouger and S. Engel

Lunar and Planetary Laboratory, University of Arizona, Tucson

R. G. Roble and B. Foster

National Center for Atmospheric Research, High Altitude Observatory, Boulder, Colorado

(JGR) July 25, 2000

Comparative terrestrial planet thermospheres

3. Solar cycle variation of global structure and winds at solstices

S. W. Bouger and S. Engel

Lunar and Planetary Laboratory, University of Arizona, Tucson, Arizona

R. G. Roble and B. Foster

National Center for Atmospheric Research, High Altitude Observatory, Boulder, Colorado